JACS Au
AN OPEN ACCESS JOURNAL OF THE AMERICAN CHEMICAL SOCIETY

pubs.acs.org/jacsau Perspective

Network Formation and Physical Properties of Epoxy Resins for Future Practical Applications

Atsuomi Shundo,* Satoru Yamamoto, and Keiji Tanaka*

Cite This: *JACS Au* 2022, 2, 1522−1542

Read Online

ACCESS | Metrics & More | Article Recommendations

ABSTRACT: Epoxy resins are used in various fields in a wide range of applications such as coatings, adhesives, modeling compounds, impregnation materials, high-performance composites, insulating materials, and encapsulating and packaging materials for electronic devices. To achieve the desired properties, it is necessary to obtain a better understanding of how the network formation and physical state change involved in the curing reaction affect the resultant network architecture and physical properties. However, this is not necessarily easy because of their infusibility at higher temperatures and insolubility in organic solvents. In this paper, we summarize the knowledge related to these issues which has been gathered using various experimental techniques in conjunction with molecular dynamics simulations. This should provide useful ideas for researchers who aim to design and construct various thermosetting polymer systems including currently popular materials such as vitrimers over epoxy resins.

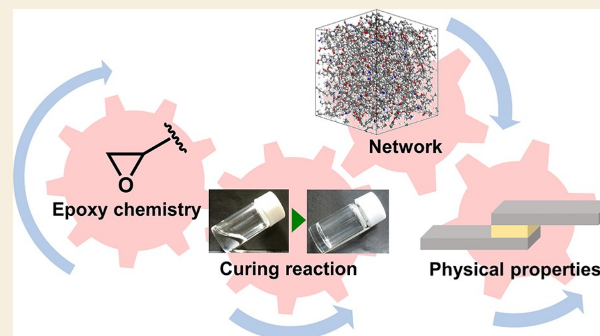

KEYWORDS: *thermoset, cross-linking, network, glass, interface, adhesive*

Downloaded via 195.252.220.185 on December 27, 2023 at 17:22:17 (UTC).
See https://pubs.acs.org/sharingguidelines for options on how to legitimately share published articles.

1. INTRODUCTION

In 1907, Leo Baekeland synthesized a phenol−formaldehyde resin, so-called Bakelite,[1] as the first example of a class of thermosetting polymers.[2] Thermosets are generally formed from a liquid mixture of monomer molecules, having multifunctional groups, which can react with each other to cross-link three-dimensionally. One of the advantages of thermosets over thermoplastics is that their precursor can be a reaction mixture having low viscosity, which offers good processability in injection and molding.[3] Epoxy resins are one of the most versatile categories of thermosets derived from the precursor having oxirane or epoxy groups. They were discovered in 1939 by Prileschajew.[3] Thanks to their excellent thermal and mechanical properties, epoxy resins have been widely applied in a range of fields.[4−6] The global market for epoxy resins is driven by the increasing demand in the fields of chemistry, automotive, aerospace, civil engineering, leisure, electrical, marine, and many others.[7]

Epoxy resins can be commonly obtained by chemical reactions of epoxy compounds with initiators or curing agents (hardeners). The high reactivity of the epoxy groups toward a wide variety of functional groups has attracted much attention from chemists as well as chemical engineers. So far, the reaction kinetics for various types of epoxy compounds, initiators, and curing agents have been examined.[8] On the other hand, researchers working with polymer materials have focused on the relationship between the network structure and physical properties. In particular, gaining an understanding of the network formation and the change in physical states (liquid, rubbery, and glassy solids) involved in the reaction process has been the subject of intensive research for many years.[9]

Epoxy resins are generally a glass-forming material and are often in a glassy state at room temperature. The mechanical relaxation associated with the network architecture of fully cured epoxy resins has been extensively studied.[10] Notably, direct characterization of the network architecture is difficult or even impossible because of their infusibility at higher temperatures and insolubility in organic solvents. These difficulties are particularly acute for the "buried" interface, at which the epoxy resins come into contact with a solid. Therefore, atomistic and coarse-grained molecular dynamics (MD) simulations are considered to be a powerful analytical tool.

From this perspective, we highlight important aspects that should be considered in current research trends. First, we briefly introduce the chemistry of epoxy groups. Then the

Received: February 22, 2022
Revised: May 24, 2022
Accepted: May 24, 2022
Published: June 9, 2022

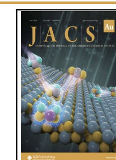

© 2022 The Authors. Published by American Chemical Society

https://doi.org/10.1021/jacsau.2c00120
JACS Au 2022, 2, 1522−1542

reaction kinetics associated with the network formation and the physical state change are presented. The network and physical properties including dynamic heterogeneity of the fully cured epoxy resins are discussed. Finally, we summarize recent applications in the practical and industrial fields.

2. CHEMISTRY OF EPOXY RESINS

2.1. Classification of Epoxy Resins

The term of "epoxy" is used to describe a range of monomers containing an epoxy group, while "epoxy resins" refers to a class of molecules containing at least two epoxy groups. The material obtained after the curing reaction is commonly referred to as "epoxy resin" even if it no longer contains epoxy groups. Figure 1 shows examples of widely used epoxy

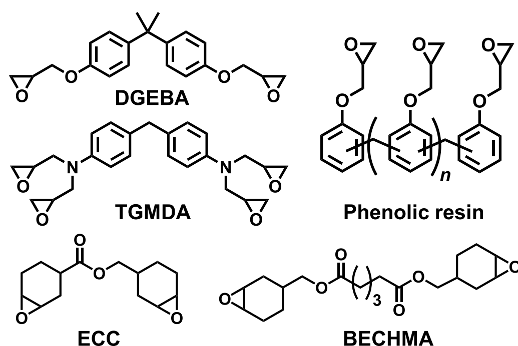

Figure 1. Typical monomers used as a precursor for epoxy resins.

monomers. Diglycidyl ether of bisphenol A (DGEBA), which can be obtained from the reaction between bisphenol A and epichlorohydrin in the presence of sodium hydroxide, is one of the most common precursors for epoxy resins.[11] Multifunctional epoxy monomers are also widely used because they tend to increase the cross-linking density.[12−15] For instance, *N*,*N*,*N'*,*N'*-tetraglycidyl-4,4'-methylenedianiline (TGMDA) is a typical monomer extensively used in aerospace composites.[16] Polyglycidyl derivatives of phenolic prepolymers are also common, known to yield epoxy resins with a higher glass transition temperature (T_g) and high resistance to thermal degradation.[17,18] Cycloaliphatic resins are another class of epoxy resins of great interest.[19,20] They have less tendency toward yellowing than aromatic resins.[21] In addition, their low viscosity and electrical loss properties have made them useful commercially in electrical and electronic applications.[22,23] Such examples can be seen for 3,4-epoxycyclohexylmethyl 3,4-epoxycyclohexanecarboxylate (ECC) and bis[3,4-epoxycyclohexylmethyl] adipate (BECHMA).

2.2. Type of Reactions and Curing Agents

An oxirane in an epoxy monomer is a class of three-membered ring. Such a small ring exhibits high reactivity dominated by the effect of ring strain, whose strain energy is estimated to be about 115 kJ·mol^{-1}.[24] Thus, epoxy monomers can generate a cross-linked network structure by either chain-growth ring-opening polymerization or step-growth polymerization, depending on the type of curing agent.[25,26] Chain-growth ring-opening polymerization can be further classified into cationic and anionic polymerizations.

Panel a of Figure 2 shows the scheme for cationic polymerization of epoxy monomers. The propagation reaction proceeds via an active oxonium at the end of the growing

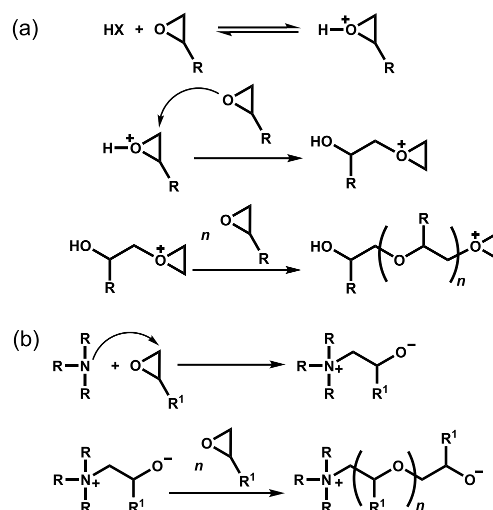

Figure 2. Reaction schemes of chain-growth ring-opening polymerization with (a) cationic and (b) anionic modes.

chain. Common initiators are boron trifluoride (BF_3) complexes[27,28] and onium salts including diaryliodonium, triarylsulfonium, or phosphonium salts.[29−32] Panel b of Figure 2 shows the scheme for anionic polymerization which is generally initiated by imidazoles[33] or highly reactive tertiary amines.[34] It is based on the formation of alkoxide, which then reacted with an epoxy monomer, leading to the generation of another alkoxide. In recent years, several authors have reported that ionic liquids such as dialkylimidazolium ions can behave as an initiator.[35] Here, it is noteworthy that epoxies can be copolymerized with other cyclic monomers. In particular, the curing of epoxy−anhydride formulations, using tertiary amines as an initiator, has been demonstrated as an alternating epoxy−anhydride anionic polymerization.[36−38]

The step-growth ring-opening polymerization of epoxy monomers can be performed using amines, acids, isocyanates, and mercaptans.[25,39−43] Of these, amines have been widely used. In this case, the reactivity and thereby the kinetics of the curing reaction are determined by the electrophilicity of the epoxy group and the nucleophilicity of the amino group. Panel a of Figure 3 shows the reaction scheme of epoxy monomers with an amine. A primary amino group first reacts with an epoxy group. This produces a secondary amino group that further reacts with another epoxy group and then a tertiary

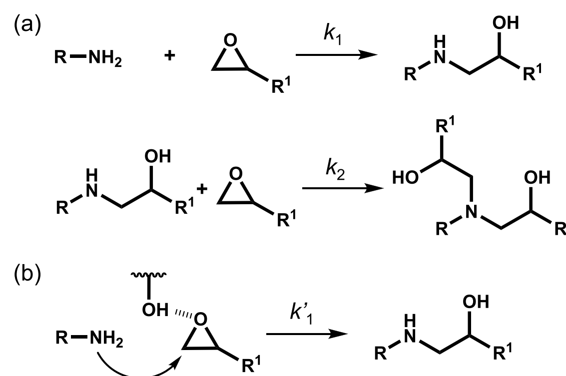

Figure 3. Reaction scheme of step growth ring opening polymerization of epoxy and amine (a) without and (b) with autocatalytic reaction. Panel b only shows the first step reaction.

https://doi.org/10.1021/jacsau.2c00120
JACS Au 2022, 2, 1522−1542

amino group is generated.[44] Since the resultant tertiary amino group gives a branching or cross-linking structure, the amines used are often referred to as "curing agents" or "hardeners". Here, it should be noted that a hydroxy group generated by the ring-opening reaction can form a hydrogen bond with an oxygen atom in unreacted epoxy monomers.[45] The formation of the hydrogen bond promotes the nucleophilic attack of an amino group to an epoxy group, as shown in Figure 3b. Such a reaction has often been regarded as an "autocatalytic reaction" and has been extensively studied.[46,47]

A wide variety of amines have been used as curing agents for epoxy resins,[25] and Figure 4 shows some common examples.

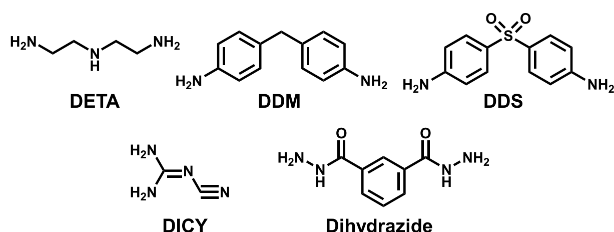

Figure 4. Typical hardeners used for epoxy resins.

Basically, aromatic amines such as 4,4'-diaminodiphenylmethane (DDM) and 4,4'-diaminodiphenylsulfone (DDS) are less reactive than aliphatic ones (diethylenetriamine, DETA) because of the weaker nucleophilicity of the epoxy groups. Dicyandiamide (DICY) is one of the most commonly used "latent" curing agents, which do not react with an epoxy monomer unless the temperature increases.[48] DICY is a solid with a high melting temperature of ca. 460 K and is insoluble in most epoxy monomers at room temperature. Thus, a mixture of DICY and epoxy monomer has excellent stability and can be cured once the temperature exceeds the melting point.[49] Such a feature leads to a long storage lifetime and makes it easier to handle.[50] As an alternative to DICY, dihydrazides are also known as a latent curing agent. Most dihydrazides can be dispersed as a solid in a liquid epoxy monomer because they possess a high crystalline feature. In addition, the nucleophilicity of amino groups is moderately reduced by the directly adjacent NH group.[51] Notably, dihydrazides with various chemical structures, which are easily obtained from the corresponding diacids, are available.[25]

To obtain a single-phase system with latent properties, several researchers have proposed the protection and deprotection of amino groups in the curing agents.[52,53] For instance, a ketone-based imine has been developed as a water-initiated latent agent.[54] Figure 5 depicts the regeneration of an

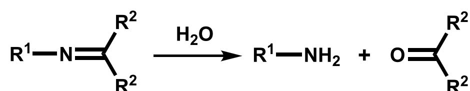

Figure 5. Regeneration of an amine by imine hydrolysis after exposure to atmospheric humidity.

amine from a ketimine. The nucleophilicity of the ketimine is low enough for a long shelf life although it is an enamine–imine tautomerism.[55] Once the ketimine is exposed to atmospheric moisture, the imine hydrolysis regenerates amine, which can react with epoxies followed by the curing reactions.[56] The nucleophilicity control of amines based on the protection/deprotection approach has been demonstrated with 2-nitrobenzyl carbamates,[57,58] *O*-acyloximes,[59] and *N*-aryl-*N*,*N'*-dialkyl urea.[60] One of the interesting approaches is a thermally activated single-component system proposed by Fréchet and co-workers, as shown in Figure 6.[61] The single

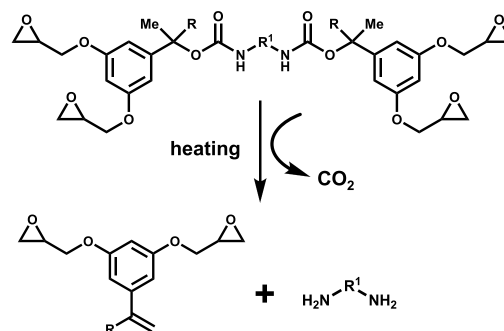

Figure 6. Single-component curing system which can generate both epoxy and amine upon heating.

precursor for epoxy resin contains both epoxy and diamine groups held by thermally degradable carbamate linkages. The precursor molecule has a long shelf life at room temperature. Upon heating, carbamate decomposition provides the eliminated alkene with epoxy groups, primary diamines, and carbon dioxide, leading to the curing reaction of epoxies with amine.[61]

3. CURING PROCESS

3.1. Reaction Kinetics

As stated in the previous section (Figure 3), the curing process based on the step growth polymerization of epoxy and amine involves two steps. At the initial stage of the curing process, small chains with linear or branched structures are formed, and this is accompanied by a gradual increase in molecular weight. As the reaction proceeds, the branching of the chains becomes more pronounced, resulting in gelation.[62] The curing time, or reaction conversion, at which gelation occurs, is called the gel point. At this point, the three-dimensional network expands over the entire system and thus the average molecular weight can be regarded to be infinity.[63] When the curing temperature is sufficiently low, the transition from a liquid or gel to a glass, so-called vitrification, is thought to take place.[64] Both the gelation and vitrification suppress further curing reactions due to a lowering of local mobility of unreacted functional groups and/or chain segments. Therefore, the curing proceeds via the chemically controlled reactions at the initial stage, followed by the diffusion-controlled reactions.[65,66]

The chemical reaction and concurrent increase in the average molecular weight at the initial stage of the curing process can be discussed on the basis of nuclear magnetic resonance (NMR) spectroscopy[67,68] and gel permeation chromatography (GPC).[69,70] However, these techniques cannot be applied to the late stage because of the insolubility of the curing product into organic solvents. Thus, differential scanning calorimetry (DSC) has been shown to be a valuable tool for studying the reaction kinetics of epoxy resins.[71,72] It is known that the reactions involving the ring-opening of epoxy groups are exothermic. Given that the reaction rate is proportional to the heat flow, the degree of the curing reaction, namely the reaction conversion (α), can be examined as a function of time. There are essentially two types of

https://doi.org/10.1021/jacsau.2c00120
JACS Au 2022, 2, 1522−1542

experiments to determine the α value. One is an isothermal experiment where temperature is kept constant.[73] The other is a "non-isothermal" or "dynamic" experiment, which involves ramping the temperature to a given value at a constant rate. For the former experiment, the α can be determined by the ratio of the heat recorded up to a certain time ($Q(t)$) to the total heat recorded over the entire reaction (Q).[73] Hence, the conversion curve, which is a plot of the α value against curing time, can be analyzed with a kinetic model, as described later. Figure 7 shows typical examples of the conversion curves at various curing temperatures.

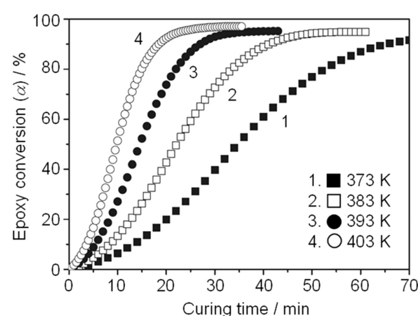

Figure 7. Typical conversion curves for a mixture of DGEBA and DDM at various curing temperatures. Data are taken from ref 73 with a style modification. Copyright 2013 Elsevier.

Fourier-transform infrared (FT-IR) spectroscopy has also been widely used for the study of epoxy−amine reaction kinetics.[74,75] In general, the reaction is monitored on the basis of the change in the intensity of the absorption bands in the near IR wavenumber range, typically 4000−7500 cm^{-1}.[76] Figure 8 shows an example of FT-IR spectra for an epoxy−amine mixture at various stages of the curing process. At the initial stage, the spectrum provides an absorption band due to the combination of the stretching and bending vibration modes of epoxy groups at ~4530 cm^{-1} (ν_{epoxy}).[75,76] Also, two bands are observed at ~4940 and ~6540 cm^{-1}. The former is assignable to the combination of the stretching and bending vibrations of primary amino groups (ν_{amino}), while the latter includes the overtones of the stretching vibration for both primary and secondary amino groups (ν_{ps}).[77] As the reaction proceeds, the absorbance for both ν_{epoxy} and ν_{amino} bands decreases, meaning that the primary amino and epoxy groups reacted with each other. The reaction is also accompanied by a change in the ν_{ps} band. The absorbance of the ν_{ps} band initially decreases and subsequently shifts toward the lower wavenumber side because of the generation of secondary amino groups. Then the absorbance decreases as a result of the transformation of secondary into tertiary amino groups.[77] Notably, a new broad band at ~7100 cm^{-1} appears as the reaction proceeds. This band corresponds to the overtone of the stretching vibration for hydroxy groups, which was generated as a result of the ring opening of epoxy groups.[77]

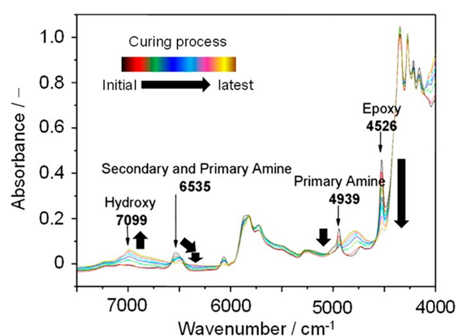

Figure 8. FT-IR spectra obtained for the reaction mixture of hydrogenated DGEBA (HDGEBA) and poly(3-aminopropylmethyl)-siloxane at 343 K. Data are taken from ref 76 with a style modification.

Based on the absorbance change in the ν_{epoxy} band, the α value can be extracted. The plot of α against curing time can be analyzed on the basis of the kinetic models, which are also applied to the DSC data.[78] The basic rate equation in the kinetic analysis can be expressed by $d\alpha/dt = k(T)f(\alpha)$, where $d\alpha/dt$ is the rate of conversion, $k(T)$ is a reaction rate constant, and $f(\alpha)$ is a function of α. The $k(T)$ is dependent on the temperature and is generally assumed to be of the Arrhenius form with a pre-exponential factor, A, and an apparent activation energy, E_a. To date, various types of kinetic models with modified $k(T)$ and $f(\alpha)$ have been proposed.[79] Of these, the Kamal−Sourour model is the most widely used for the epoxy−amine reactions.[80] In this model, the autocatalytic reaction of epoxy groups with primary amino ones is considered. This model represents the chemically controlled kinetics at the initial state of the curing reaction. To account for the shift from chemically controlled to diffusion-controlled reactions, the model has to be modified.[81] For instance, Dušek and Havlíček introduced a dependency of the reaction rate on the T_g for the curing system.[82] Another approach to take the diffusion effect into account is expanding the reaction kinetics model with a diffusion factor.[83,84]

An advantage of the kinetic study of the curing reaction with FT-IR over DSC is that the concentration of epoxy groups (C_E), primary (C_{A1}), secondary (C_{A2}), and tertiary amino groups (C_{A3}) can be determined. The analytical method proposed is based on the assumption that there are two step reactions as shown in Figure 3a without any side reactions and the reactivity ratio (R), which is defined as the reaction rate constant ratio between first and second steps (k_2/k_1), is independent of the reaction path.[85,86] Thus, considering the mass balance of the functional groups, the concentration of each group can be estimated on the basis of the absorbance change for the ν_{epoxy} and ν_{amino} bands. Figure 9 shows an example of the time course of C_E, C_{A1}, C_{A2}, and C_{A3} during the curing reaction process. As the reaction proceeds, the C_E and C_{A1} values decrease while the C_{A2} and C_{A3} values increase. Then the C_{A2} value starts to decrease, while C_{A3} keeps increasing before finally reaching a plateau. The plateau region

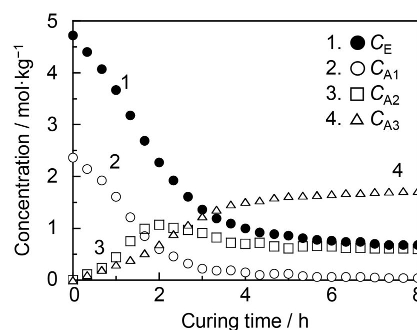

Figure 9. Time course for C_E, C_{A1}, C_{A2}, and C_{A3} during the curing process at 323 K. Data are taken from ref 88. Copyright 2020 Royal Society of Chemistry.

https://doi.org/10.1021/jacsau.2c00120
JACS Au 2022, 2, 1522−1542

corresponds to the diffusion-controlled reaction due to the gelation and/or vitrification.[87,88] According to a suggestion by PazAbuin et al., the R value can be estimated from the concentration ratio between C_{A1} and C_{A2} at the curing time, at which C_{A2} is maximized.[89] The R values so far reported are less than 0.5, meaning that the reactivity of secondary amino groups is much lower than that of primary ones.[89] This is explained by the reduced nucleophilicity and the increased steric hindrance of a secondary amino group relative to a primary one.[85,86]

3.2. Evolution of Network Structure

As mentioned before, FT-IR spectroscopy provides information on the change in the concentration of functional groups during the curing process. Based on such a change, the network formation can be discussed. It has been pointed out that the generation of secondary and tertiary amino groups in an epoxy−amine mixture depends on the curing temperature.[87] At a lower temperature, secondary amines are initially generated and then converted to tertiary ones. At a higher temperature, on the other hand, the secondary and tertiary amines are concurrently generated at the initial stage of the curing. To explain such conversion behaviors, two different types of epoxy−amine network formation were proposed by Morgan and Sahagun.[90] Figure 10 shows a schematic

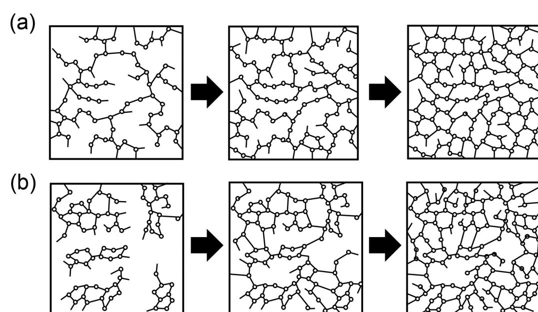

Figure 10. Pictures for network formation for the curing at (a) lower and (b) higher temperatures. Reproduced with permission from ref 88. Copyright 2020 Royal Society of Chemistry.

illustration showing the two different network formations. At a lower curing temperature, linear chains initially grow until a low-density network expands over the system (skeleton network), and then unreacted groups cross-link within the skeleton network. The curing at a higher temperature provides the initial generation of the cross-linked domains, or microgels, followed by the interconnection with one another. The former and latter types would lead to less heterogeneous and heterogeneous networks, respectively.[88]

Direct investigation of how the network structure in an epoxy resin develops during the curing process is quite difficult or even impossible because of the infusibility at higher temperatures and the insolubility in organic solvents. Generally, the resin has to be fractured and then characterized. Atomic force microscopy (AFM) and scanning electron microscopy (SEM) and have been commonly used to analyze the aggregation states for the fracture surface.[91−96] It has been pointed out that the fracture surface of an epoxy resin contained nodules with a size ranging from tens to hundreds of nanometers.[92−94] The nodular structure has been regarded as being at relatively high cross-linking regions with an interstitial phase of low cross-linking density. Also, it has been found that the characteristic length of the nodules decreases with increasing curing time.[95] Such a morphological change was thought to reflect the increase in the cross-linking density as a result of the curing. Here, it should be noted that there is another interpretation for the nodular structure. That is, the nodular structure itself is not proof for the difference in the cross-linking density of the network because a similar structure is also found for the fracture surface of polymers without any cross-links.[91,96] However, the latter interpretation seems to have been invalidated by a recently developed technique, nanoscale infrared analysis (AFM-IR). In this technique, the deflection of an AFM probe is used as a local sensor to detect photothermal expansion in response to infrared excitation, and the nanoscale lateral variations are detected in response to the illumination at different wavenumbers.[97] AFM-IR measurement has revealed that the nodular structure corresponds to the chemical heterogeneity associated with the heterogeneous cross-linking structure.[98,99]

Recently, Izumi and Shibayama et al. proposed a non-destructive method using small-angle X-ray and neutron scattering (SAXS and SANS) to characterize the network at various state of the curing for a phenolic resin.[100−102] In this method, the resin is swollen in a good solvent to enhance a spatial difference in the cross-linking density.[103] Through a series of works, it was found that tightly cross-linked domains initially appeared, and then the size of the domains increased as a result of incorporating other polymer chains into the domain.[98] Such a network formation was also the case for epoxy resins.[104]

3.3. Change in Physical Properties

Gillham et al. proposed time−temperature-transformation (TTT) diagram, where gelation, vitrification, as well as degradation are represented.[105] Figure 11 shows a typical

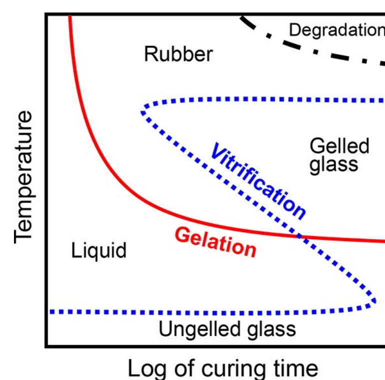

Figure 11. Typical time−temperature transformation (TTT) diagram for thermosetting polymers including an epoxy resin. Reproduced with permission from ref 105. Copyright 2003 John Wiley and Sons.

TTT phase diagram for thermosets including epoxy resins. It contains the gelation (solid, red), vitrification (dotted, blue), and degradation curves (dashed-dotted, black) at borders between different phases as functions of curing time and temperature. Liquid (before gelation), rubber (after gelation but above T_g), gelled glass (after gelation and below T_g), and degraded polymer are possible phases. The curing temperature is commonly chosen on the basis of the TTT diagram. No matter what temperature is chosen, the system will go through the gelation and/or the vitrification curve(s) after a certain time. Thus, great efforts have so far been made to gain a better

https://doi.org/10.1021/jacsau.2c00120
JACS Au 2022, 2, 1522−1542

understanding of gelation and vitrification during the curing process.[106,107]

The reaction conversion at which the macroscopic gelation occurs, or the gel point, is usually determined by gel fraction measurement. Once a reaction system reaches the gel point, the insoluble component appears even in a good solvent, and then the fractional amount increases with increasing curing time.[108] Viscosity measurement is also common for determining the gel point. The steady-state shear viscosity is measured as a function of curing time. Once the system undergoes gelation, the viscosity increases with increasing time. By extrapolating the viscosity to infinity, the gel point can be determined.[109]

Dynamic shear oscillatory measurements have become more common in characterization of the gel point upon the curing process.[110−112] Figure 12 shows a typical example for the time

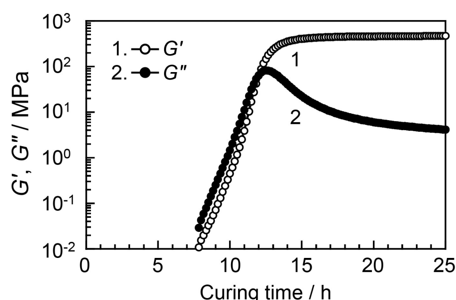

Figure 12. Time course of G' and G'' during the reaction between HDGEBA and 1,4-cyclohexanebis(methylamine) (CBMA) at 296 K. Data are taken from ref 104. Copyright 2019 American Chemical Society.

course of shear storage and loss moduli (G' and G'') during the curing process of an epoxy resin. The measurement was performed at an angular frequency of 10 rad s^{-1}, which has been commonly used according to the suggestion by the American Society for Testing and Materials (ASTM).[113] At the initial curing stage, G'' was larger than G', indicating a liquid state. As curing proceeded, both G' and G'' increased before reaching to a crossover point, at which G' and G'' became identical with each other. After that, G'' reached a maximum while G' kept increasing and then approached a plateau. The crossover point of G' and G'' is often regarded as the gel point.[114] However, since the crossover point depends on the measurement frequency, determination of the gel point using tan δ (= G''/G') should be made with care. Actually, the gel point was determined to be the time at which the tan δ curves acquired at various frequencies intersect one another.[115,116] Here, it is noteworthy that the decrease in G'' with increasing time is an indication of vitrification, where the segments are frozen in terms of mobility, leading to the lesser contribution of the energy dissipation.[115,116] In fact, when the curing temperature is substantially higher than the T_g of the system, no decrease in G'' is observed during the curing process.[117] The T_g value, which generally increases with increasing curing time, can be determined as a heat capacity change detected by temperature-modulated differential scanning calorimetry (TMDSC).[118,119]

Characterization methods for the change in physical properties of the epoxy resins during the curing process are often limited to bulk measurements, which provide ensemble-averaged information over the entire region of the system. Recently, we applied a particle tracking experiment, which is one of the techniques for microrheology, to an epoxy−amine curing system.[104] In this technique, probe particles are embedded in the medium to be measured. Since the thermal motion of the particles reflects the physical properties of the surrounding medium, tracking the movement provides insights into the local properties of the medium.[120,121] Information on the spatial heterogeneity can be obtained by detecting the particles located at different positions in the medium.[122,123] Also, by changing the particle size, the length scale of the observation can be altered.[124−128] Figure 13 shows an

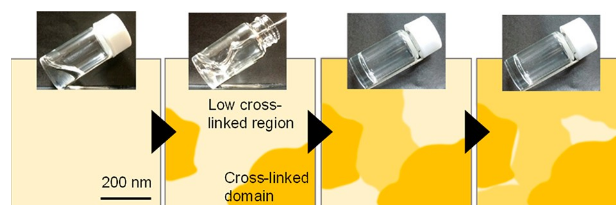

Figure 13. Schematic illustration showing the evolution of the heterogeneity during the curing process. Reproduced from ref 104. Copyright 2019 American Chemical Society.

illustration of the curing process drawn after a particle tracking study. Observation of individual particles at different locations revealed that, at the initial stage of the curing, the heterogeneous structure with a mesoscopic scale was generated and the characteristic length scale decreased with increasing curing time.[104] Such a picture was recently confirmed by bimodal AFM, where both modulus and dissipated energy quantities describing the elastic and adhesive responses, respectively, were simultaneously obtained.[129] Notably, the length scale of the heterogeneity decreased to a value of ∼10 nm at the fully cured stage.

3.4. Molecular Picture of Structure Formation

Atomistic and coarse-grained MD simulations have been applied to model the cross-linked structure of epoxy resins since around the year 2000. These developments have enabled us to gain access to the reaction kinetics, heterogeneity, and thermal and mechanical properties of the resins.[130−133] The basic procedure for creating the cross-linked structure is as follows. Sites where epoxy and amine molecules react are specified in advance, and then, when they approach within a certain distance during the MD simulation, the chemical bonds are reorganized and reacted. Yarovsky and Evans developed a modeling method for the cross-linked structure of a water-soluble phosphated epoxy resin.[134] The distance to create new chemical bonds was set to within 0.6 nm, while at the same time, produced water or alcohol molecules were removed from the system. Wu and Xu proposed a method of reacting in order from the closest pair existing in the range of 0.4−1.0 nm and achieved a high reaction conversion of 90% or more.[135] Komarov et al. proposed a method to improve computational efficiency by running the coarse-grained (CG) model once. In their method, the all-atom model is first converted to a CG model to reduce the computational load, and the curing reaction is simulated using CGMD. The obtained structure is then remapped to the all-atom model.[136] Varshney et al. proposed a procedure to obtain a highly dense system with a reaction conversion of about 90% by differentiating the reactivity of primary and secondary amines.[137] Bandyopadhyay

https://doi.org/10.1021/jacsau.2c00120
JACS Au 2022, 2, 1522−1542

et al. used a united atom model for a computationally efficient method.[138]

The methods described so far proceed in many steps, that is, in order from the closest one, and are effective for reducing the local stress in the system.[139] On the other hand, there is another way in which pairs that may chemically react are specified in the initial structure and reactions are carried out in a single step.[140] Although the computational efficiency of this approach has advantages, it is difficult to obtain a sufficiently relaxed structure. Lin and Khare proposed a single step method to obtain a relaxed structure by using a simulated annealing algorithm to minimize the sum of the bond length.[141]

The charge of each atom must be renewed when the chemical bond recombination occurs due to the cross-linking reaction. Generally, for the sake of simplicity, the electrical charge of atoms determined by the force field is assigned or calculated via a simple method like charge equilibration (QEq).[142] Li and Strachan used the electronegativity equalization method (EEM), a fast empirical method that imparts a charge dependent on the surrounding environment. This made it possible to create a more precise cross-linked structure.[143] Since the cross-linking reaction between epoxy and amine is exothermic, the temperature rises as the reaction progresses. Okabe et al. proposed an elegant algorithm that considers the activation energy of the reaction and the heat generated by the curing reaction, as shown in Figure 14.[144] The Arrhenius-type

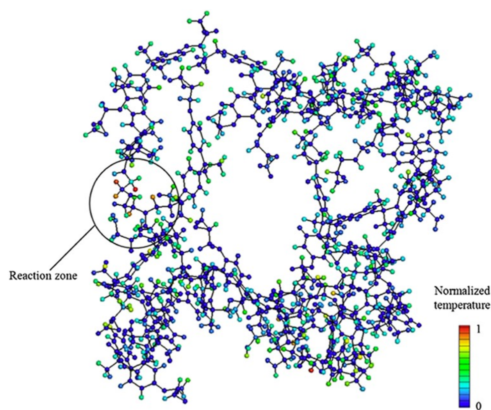

Figure 14. DGEBA-based network structure and temperature distribution showing the rise in local temperature due to the exothermic reaction. Reproduced with permission from ref 144. Copyright 2013 Elsevier.

reaction probability including the activation energy and the local temperature is defined, and whether or not the reaction occurs is determined by comparing with a random number. Once the reaction occurs, the kinetic energy corresponding to the heat of formation is applied to the site involved in the reaction, the temperature rises momentarily, and the subsequent reaction is accelerated. This method has made it possible to investigate differences in kinetics depending on the molecular structure.[145]

Based on the heat generated by the reaction using Okabe's method, the heterogeneity of the network observed in the reaction process can be explained. We discussed the origin of the mesoscopic heterogeneity generated in an epoxy resin on the basis of the MD simulation.[104] That is, once a reaction occurs, the temperature at the site is locally elevated, and a subsequent reaction is accelerated, resulting in the formation of the spatial heterogeneity.

We studied the effect of the molecular size of epoxies and amines on the reaction kinetics.[146] In the combination of larger and smaller molecules of epoxy and amine, it was seen that the smaller the epoxy the faster the reaction. This is because when a primary amine reacts to become a secondary amine it is incorporated into the network, so that even if the initial diffusion is fast, the movement becomes slow. Also, we showed that the density increased due to the shrinkage as the reaction progressed; however, the shrinkage hardly occurred beyond the gel point.[147] On the other hand, it was found that many free spaces in which water molecules can enter are formed beyond the gel point, as shown in Figure 15. It was ascertained that absorbed water molecules exist in the free space forming hydrogen bonds and diffuse in the free space one after another.

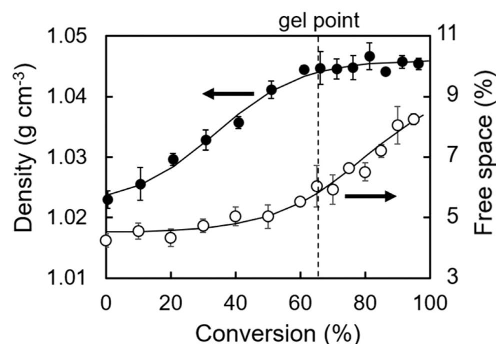

Figure 15. Changes in density and free space occupancy during the curing process. Data are taken from ref 147. Copyright 2021 Royal Society of Chemistry.

4. NETWORK AND PHYSICAL PROPERTIES

4.1. Cross-Linking Density and Thermal Motions

One of the outstanding features of epoxy resins is the facile tunability of the network architecture by changing the cross-linking density. For example, the cross-linking density has been adjusted by changing the stoichiometric ratio of epoxy and amine in the initial reaction mixture.[148,149] However, this method alters not only the cross-linking density but also the number density of residual functional groups and thereby the network defects including dangling chains, in which one end attaches to the network and the other is free.[150] An alternative approach to changing the cross-linking density is the use of a mixture of mono- and difunctional amines as a curing agent. In this method, monofunctional amines behave as a chain extender, and thus, the cross-linking density can be systematically varied on the basis of the ratio between the mono- and difunctional amines.[151,152] Furthermore, the cross-linking density can be simply tailored by varying the molecular weight of difunctional epoxies and/or amines. If a full conversion is ideally reached, this method should yield a network which contains no dangling chain.[153] Thus, the distance between the two functional groups in epoxies or amines corresponds to the chain length between the cross-linking points.[154,155]

Cross-linking density affects the physical properties of epoxy resins. For example, as the cross-linking density increases, the T_g also increases.[155,156] This is generally explained in terms of the dense glassy state, in which network chains tightly pack together, leading to a reduction in the free volume.[157,158] If

dangling chains exist in the network, the T_g tends to decrease because chains can be actively moved within a certain part of the free space.[159] The effect of change in the architecture of the epoxy−amine network on the free volume content has been studied using positron annihilation lifetime spectroscopy (PALS).[160,161] PALS is an analytical technique that can quantify nanoholes on the order of 0.2−2.0 nm in diameter, which are consistent with the interchain dimensions of most polymers.[160] Pujari et al. reported that the free volume fraction increased with increasing cross-linking density although the size decreased.[162] This is in good accordance with the result shown in Figure 15. Besides, it should be noted that the effect of the free volume content associated with the local chain motion on the moisture uptake of the epoxy−amine network has been elegantly described by Soles et al.[163] and more recently by other researchers.[164,165] Such an approach provides useful knowledge regarding hydrothermal aging, which is one of the degradation phenomena due to the presence of moisture at an elevated temperature.

Thermal molecular motion in epoxy resins was also dependent on the cross-linking density, as evidenced by dielectric relaxation spectroscopy (DRS)[166,167] and dynamic mechanical analysis (DMA).[168,169] Figure 16 shows temperature dependence of tensile storage (E') and loss moduli (E'') for an epoxy resin composed of DGEBA and 1,2-diaminoethane (DAE) by DMA. Two E'' peaks were observed at around 420 and 250 K. The first peak at 420 K was accompanied by a clear decrease in E'. The peak was referred to as α-relaxation which was generally assigned to the segmental motion in the network.[170] The latter peak at 250 K was named β-relaxation, which mainly corresponded to the motion of diphenylpropane groups and glyceryl units, $-CH_2-CH(-OH)-CH_2-O-$.[171,172] Since the shape and intensity of the β-relaxation peak was affected by the cross-linking density, it was noted that the relaxation also contained a local motion coupled with the motion of the main chain in the network. The amplitude of the β-relaxation has been discussed in conjunction with the stiffness of the glassy epoxy resins.[173]

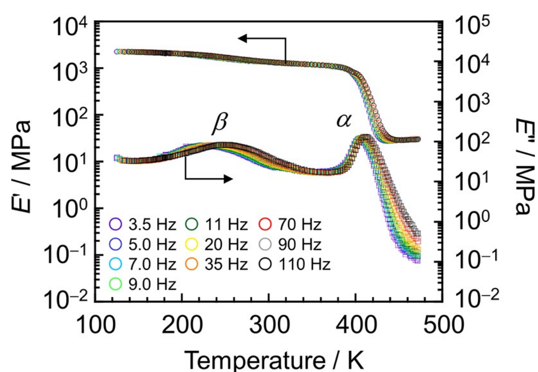

Figure 16. Temperature dependence of E' and E'' for an epoxy resin composed of DGEBA and DAE at various frequencies ranging from 3.5 to 110 Hz. These are unpublished data.

4.2. Dynamic Heterogeneity

Since epoxy resins are often in a glassy state at room temperature, the network structure is frozen in terms of its mobility. Thus, understanding the glass transition dynamics associated with cross-linking density is needed to regulate the mechanical properties such as yielding and fracture behaviors.[174,175] The glassy dynamics can be characterized by the fragility index (m), which is defined as the apparent activation energy for the α-relaxation process near the glass transition.[176] Figure 17 shows a semilogarithmic plot of relaxation time (τ) for the α-relaxation process against the inverse temperature (T^{-1}) for epoxy resins with different cross-linking densities. The abscissa is normalized by each T_g value, provided as an Angell plot.[176] The m value corresponds to the steepness of the plot at T_g. Combining with an incoherent elastic neutron scattering technique, the magnitude of m is claimed to be the extent of the dynamic heterogeneity, which is a transient spatial fluctuation in the cooperative segmental dynamics near the glass transition.[177] Based on the m value, the extent of the dynamic heterogeneity can be discussed.[177] The glass transition dynamics can be also characterized by characteristic length scale of the cooperative rearranging region (CRR) (ξ_{CRR}).[178−180] The CRR is defined as the smallest subsystem in which one segment is necessarily involved in coordinated motions of other segments at a temperature near T_g.[178−180] The ξ_{CRR} value can be experimentally estimated by various techniques such as low-frequency Raman spectroscopy,[181,182] Brillouin light scattering,[183,184] four-dimensional NMR spectroscopy,[185,186] and TMDSC.[187,188] Some studies have reported that with increasing cross-linking density in the epoxy resin, the m and ξ_{CRR} values increased, while others decreased.[162,189]

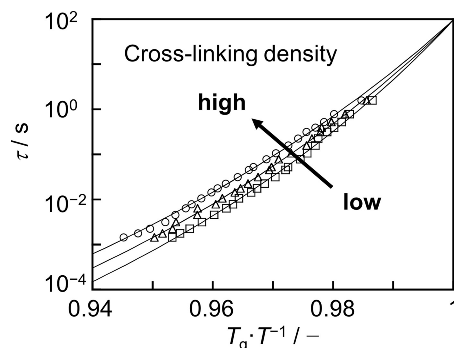

Figure 17. Angell plots for epoxy resins with various cross-linking densities. Symbols and solid lines denote experimental data and best-fit curves using the Vogel−Fulcher−Tammann equation, respectively. Data are taken from ref 155. Copyright 2021 American Chemical Society.

Recently, we studied the glass transition dynamics in epoxy resins in which the cross-linking density was systematically altered by chain length of n-alkyl diamines used as curing agent.[155] As the cross-linking density increased, the T_g increased, accompanied by a reduction in ξ_{CRR} and an increase in the dynamic heterogeneity. Notably, the analysis of the self-part of the space-time correlation function by the MD simulation revealed that the thermal motion of nitrogen atoms, which acted as a cross-linking point, was suppressed in comparison with that of other constituent atoms. The motional difference between nitrogen and other atoms, which corresponded to the dynamic heterogeneity, became more significant as cross-linking density increased. In addition, by applying a time−temperature superposition (TTS) principle to the dynamic viscoelastic functions, we found that as the cross-linking density increased, the thermal expansion of the free volume was suppressed and the entropic elasticity became less remarkable in the temperature region above the T_g.[190] With

the aid of MD simulation, the entropy change was confirmed by isobaric molar heat capacity calculated from the ensemble variation of enthalpy. Here it should be noted that the TTS principle is one of the promising methods to predict long-term properties from short-term tests.[191−193] Actually, the creep measurements at various temperatures, which require a time of 10 h, enable us to access a time scale of up to 10^6 h.[194] Since the long-term properties are closely related to their durability, the their prediction is of importance from a practical application perspective.[194−196]

4.3. Fracture Toughness

Epoxy resins are generally brittle. Since this feature is one of the greatest drawbacks for usage as a structural material and adhesive, it is desired to overcoming this problem. So far, many researchers have studied the fracture toughness for polymer glasses without any chemical cross-links.[197−199] Through a series of works, it is known that the toughness of polymer glasses depends on the molecular weight, or the apparent entanglement density, of chains.[197,199] This is explained in terms of the slippage of chains with others, induced by the deformation and/or craze formation.[200,201] Thus, once the chains are chemically cross-linked with one another, the chain slippage is expected to be suppressed, resulting in an improvement of fracture toughness. This strategy should work for epoxy resins but do not necessarily. In fact, it has been reported that as the cross-linking density increases, the toughness increases and then begins to decrease.[202,203] Hence, further study to obtain a better understanding of the mechanism of toughness manifestation should be conducted.

We recently reported on how curing temperature affected the fracture behavior of the resultant epoxy resins.[88] Epoxy resins were prepared by precuring at four different temperatures and then postcured to eventually reach the same cross-linking density. However, as the precuring temperature increased, the *m* value decreased. That is, the dynamic heterogeneity became more apparent. Figure 18 shows photographs of the four epoxy resins immersed in tetrahydrofuran (THF), which is a good solvent for them. It is known that once a glassy material is exposed to a good solvent, or vapor, macroscopic fractures occur due to an enhancement of residual stress.[204,205] Since the epoxy resins are often utilized in contact with a solvent, the resistance to the solvent-induced stress is required in various applications.[206] Interestingly, it was found that the immersion time required to reach fracture became shorter as the extent of the dynamic heterogeneity increased as a result of the stress concentration.[88]

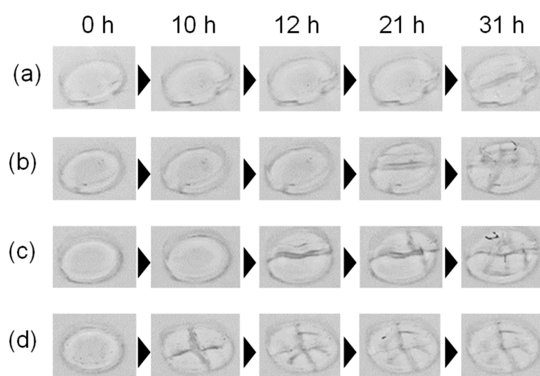

Figure 18. Photographs of four epoxy resins with different *m* values of (a) 130, (b) 110, (c) 99, and (d) 85 in THF after various immersion times. Reproduced with permission from ref 88. Copyright 2020 Royal Society of Chemistry.

In practical applications, one of the common approaches to toughening epoxy resins is to disperse soft particles as a filler into the matrix.[207−210] For example, incorporating rubbery polymer particles such as carboxy-terminated butadiene acrylonitrile can remarkably enhance the fracture toughness.[207−209] The toughening mechanism proposed is the cavitation of the rubbery particles themselves followed by void growth, which leads to energy dissipation.[208,209] Several types of nanomaterials such as carbon nanotubes, graphene, clay, and silica have also been tested.[211−214] Of these, silica particles have attracted attention because of their high specific surface area, high surface energy, low toxicity, and ease of manufacturability. Furthermore, the compatibility of silica particles into an epoxy *matrix* can be tuned by surface modification with silane coupling reagents.[215−218] Using silica particles as a filler, improvements in the toughness have been achieved.[219−222] Since silica particles can be regarded as a hard material, the toughening mechanism should differ from that based on rubbery polymer particles. After many works dealing with the effect of the size and the volume fraction of silica particles, the process related to the toughening mechanism is considered to be mainly categorized into two. One is an in-plane process such as crack tip pinning or bowing[223] and crack path deflection,[224,225] while the other is an out-plane process such as debonding and plastic void growth.[226,227]

Recently, Yamada, Kobayashi and co-workers reported *in situ* transmission electron microscopic (TEM) observation of the deformation and fracture processes for an epoxy resin film containing silica nanoparticles under the tensile process.[228] Dispersed silica nanoparticles in the composite arrested the progress of the crack tip and prevented crack propagation. Concomitantly, the generation and growth of nanovoids at the epoxy matrix/nanoparticle interfaces were clearly observed, particularly in the region near the crack tip. Also, using a digital image correlation method, the presence of particles in the growing crack suppressed the generation of strain, potentially contributing to hindering crack growth, as shown in Figure 19.

4.4. Physical Properties by Simulations

Thermal and mechanical properties have also been studied using the network structure modeled by simulations. Evaluating the change in the specific volume with respect to

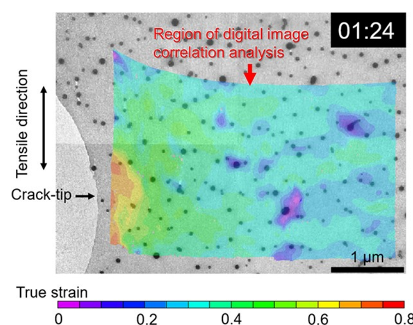

Figure 19. True strain distribution in the vicinity of the crack tip for epoxy resin composed of HDGEBA and CBMA. The tensile displacement is applied continuously in the *y* direction. The crack is expected to grow in the *x* direction. Reproduced with permission from ref 228. Copyright 2022 Royal Society of Chemistry.

https://doi.org/10.1021/jacsau.2c00120
JACS Au 2022, 2, 1522−1542

the temperature, the coefficient of thermal expansion (CTE) and the T_g can be obtained. The T_g value is defined as the temperature at which the slope of the specific volume as a function of temperature changes upon the cooling process. However, the T_g value is generally higher in an MD simulation than in an experiment because the cooling rate used in the simulation is several orders of magnitude higher than in the experiment. The difference can be corrected using the Williams−Landel−Ferry (WLF) equation. Soni et al. compared the simulated CTE and T_g values of various epoxy resins with experimental ones.[229] They also discussed the chain length effect of cross-linkers, shown in Figure 20, and pointed out that an increase in the chain length of the cross-linker led to a larger difference between the predicted and experimental values of T_g.

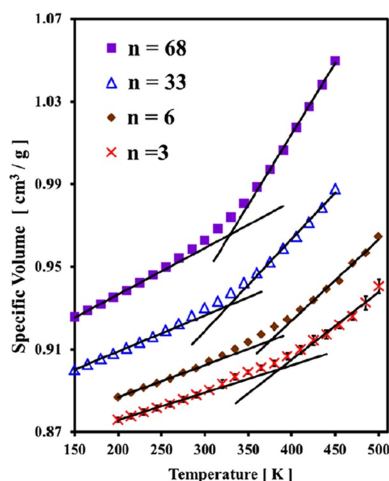

Figure 20. Example of T_g determination from the temperature dependence of specific volume for the four epoxy resins composed of DGEBA and poly(oxypropylene) diamines with the different chain lengths (n). Data are taken from ref 229. Copyright 2012 Elsevier.

Mijović and Zhang examined the local relaxation dynamics of a cured epoxy resin via DRS and discussed the molecular interaction arisen from hydroxy and ether groups based on an MD simulation.[230] Shenogina et al. estimated the elastic constants for highly cured epoxy resins and claimed that the values so obtained were higher than those by experimentation.[231] They tried to explain the discrepancy on the basis of both finite-size effect and limitation of the static deformation approach to account for the dynamic effects. Okabe et al. evaluated Young's modulus for cured products of several combinations of epoxy and amine and showed that the experimental values could be successfully reproduced after adjusting the van der Waals radius to fit the density in the experiment.[232] They also claimed that electrostatic interaction plays an essential role in the mechanical properties. Odegard et al. proposed a simulation procedure using a reactive force field, which can handle the recombination of chemical bonds, and discussed the mechanical properties for epoxy systems comparing the results with experimental ones.[233] In general, the strain rate in an MD simulation is several orders of magnitude higher than that of an experiment due to the limitation of computing time. They stated that the calculated values matched the straight line extrapolated by the experimental values, as shown in Figure 21.

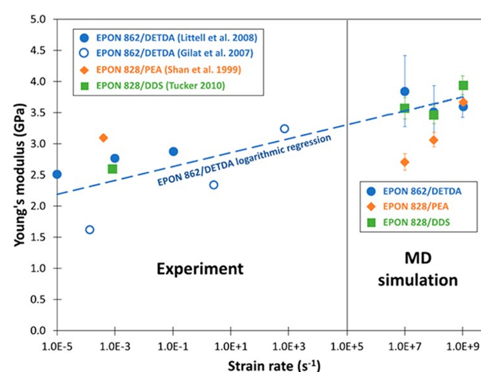

Figure 21. Relationship between strain rate and Young's modulus obtained in experiments and simulations. EPON 862: diglycidyl ether of bisphenol F (DGEBF); EPON828: DGEBA; DETDA: diethyltoluenediamine; PEA: polyetheramine. Data are taken from ref 233. Copyright 2021 American Chemical Society.

4.5. Interfacial Properties

Epoxy resins have been widely used as an adhesive in various industrial applications. Two adherend surfaces adhered by the epoxy resin can be debonded either by "cohesive" or "adhesive" failure. Cohesive failure occurs in the bulk region of an epoxy resin or in the bulk of an adherend material. Conversely, adhesive failure occurs at the interface between an epoxy resin and the adherend. Actually, the failure occurs due to a combination of both cohesive and adhesive modes.[234] In general, the cohesive mode is preferable to achieve a relatively high adhesive strength. If the strength of the interaction between the epoxy resin and the adherent surface is not high enough, adhesive failure takes place, leading to facile delamination.[234] One way to avoid this is to evaluate the strength of the chemical interaction at the interface. Experimentally, the surface free energy may be measured to estimate the adhesive force at the interface but it is not easy to measure the epoxy interface during the reaction. As an alternative method, MD and density functional theory (DFT) techniques have been used to estimate the relationship between the surface chemical states of the adherend material and the interfacial interaction. Bahlakeh and Ramezanzadeh studied the adhesion mechanism for untreated/treated steel substrates under dry and wet conditions and showed the role of electrostatic and van der Waals interactions along with the order of the surface states.[235]

It is known that the physical properties of epoxy resins near the solid interface differ greatly from those in the internal bulk region.[236] Since such an interfacial region especially contacted with a metal substrate is on (sub)micrometer scale in its thickness, it is often referred to as an "interphase".[237,238] The interface and/or interphase are/is considered to be an important factor for the material performance. Such can be seen in a flip-chip microelectronic packaging, which uses an epoxy resin as an electronical insulating adhesive. In this case, the interphase between the epoxy resin and the metal layer plays an important role in the long term durability.[239] Thus, the structure and physical properties of the interphase have been extensively studied.[240,241] For example, Carriere et al. examined the T_g value for an epoxy resin as a function of film thickness, suggesting an elevation of the T_g in the interphase contacted with a silicon substrate with a native oxide layer.[242] Chung et al. reported that using scanning force microscopy-based force modulation microcopy (SFM-FMM), the inter-

https://doi.org/10.1021/jacsau.2c00120
JACS Au 2022, 2, 1522−1542

phase consisted of a high-stiffness region near the interface with copper which was adjacent to a relatively low-stiffness region along the direction normal to the interface.[243]

A possible explanation for the interphase formation is that the chemical composition of an epoxy resin is not uniform along the direction normal to the solid interface.[244] That is, the epoxy or amine component is preferentially segregated to the interface. Other explanation includes the change in the reaction kinetics for the epoxy-amine mixture near the solid substrate due to the imbalance of the reactants,[245] the catalytic effect of metallic oxide substrate,[246] the suppressed diffusion of the reactants,[247] and so forth.[248] Using FT-IR with an attenuated total reflection (ATR) mode, we also found the initial reaction kinetics for the epoxy and amine compounds are slower near the solid interface than in the bulk region.[249]

So far, many researchers have discussed a possible formation mechanism for the interphase near the metal substrate.[250,251] If the interphase formation is a result of the preferential segregation of the amine (or epoxy) component due only to the difference in surface energy between two components, the thickness would on the order of the size comparable to that of the epoxy or amine residues. However, the thickness of the interphase has been found to be much greater than expected, although it depends on the kind of metal.[251] Previously, it has been pointed out that metal ions diffused out from the metal into the mixture of epoxy and amine and then coordinated with amine(s), resulting in the complex formation.[250] In fact, energy dispersive X-ray spectrometry (EDX) and electron energy loss spectroscopy (EELS) for a cross-section of an epoxy resin contacted with aluminum and copper substrates revealed that metal species deeply migrated into the epoxy resin.[252,253] Recently, we confirmed that an amine component was preferentially segregated near the copper interface by a nondestructive method using angular-dependent X-ray photoelectron spectroscopy (ADXPS) in which an incident X-ray was guided from the copper surface, as shown in Figure 22.[254]

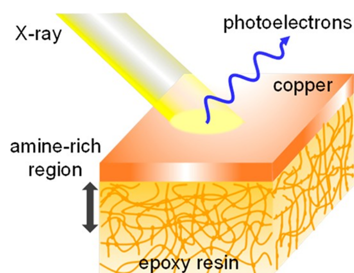

Figure 22. Schematic illustration of a nondestructive method to examine the depth profile of the chemical composition along the direction perpendicular to the copper interface. Illustration is reproduced with permission from ref 254. Copyright 2018 Springer Nature.

There are several reports on the aggregation states and the reactivity of molecules in an epoxy resin near the interface based on MD simulations. We found that in a mixture of epoxy and amine at the interface with copper amine with a smaller molecular size was selectively concentrated due to the packing entropy.[255] We further demonstrated that epoxy segregated at the interface when smaller epoxy molecules were used.[256] When larger and smaller epoxy and amine were mixed, each smaller molecule selectively segregated at the interface as shown in Figure 23. Consequently, the progress of the reaction was suppressed at the interface by the depletion of the reaction partner as well as the decrease in mobility.

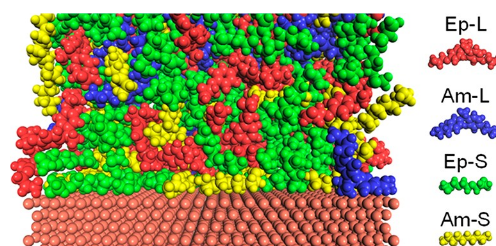

Figure 23. Representative snapshot near the interface. Molecules of DGEBA (Ep-L), 2,2-di(4-(3-aminopropyl)phenyl)propane (Am-L), ethylene glycol diglycidyl ether (Ep-S), and 1,8-diaminooctane (Am-S) are colored red, blue, green, and yellow, respectively. Here, Ep and Am denote epoxy and amine, respectively, and the letters L and S mean larger and smaller. Copper atoms are colored brown. Models are reproduced with permission from ref 256. Copyright 2021 Royal Society of Chemistry.

5. APPLICATIONS

Epoxy resins have been widely used in various applications for industrial products and home appliances to take advantage of their excellent properties. In this section, the recent trends with pioneering applications are briefly summarized.

5.1. Structural Materials and Adhesives

As mentioned in section 4.3, the toughening of epoxy resins has been strongly desired for their application as structural materials and adhesives. This has been attempted by various approaches, which are classified into (i) elastomer modification, (ii) particulate modification, (iii) thermoplastic modification, and (iv) miscellaneous methods.[210,257] Incorporating the polyrotaxane (PR) structure into epoxy resins is also a promising candidate method.[258,259] Hanafusa et al. studied the molecular dynamics of PR in which poly(ε-caprolactone) (PCL) grafted onto α-cyclodextrin (CD) crossed the poly(ethylene glycol) (PEG) axis, uniformly dispersed in a cross-linked epoxy resin.[260] As the temperature rose, PEG in PR underwent a glass-to-rubber transition that fluctuated within the glassy PCL-grafted CD confined in the matrix, causing the viscoelastic relaxation. This improved the deformability and toughness of the epoxy resin containing PR under uniaxial stretching.

The degradation of epoxy resins after use is a critical issue for material recycling, reducing the environmental load as well as the development of dismantlable adhesives. Tano and Sato reported an epoxy resin, composed of DGEBA with a photodimer of 9-anthracene carboxylic (9-AC) acid,[261] which was successfully decross-linked to be solubilized in organic solvents upon heating. The solubilized products reformed a network structure by photodimerization of 9-AC units. Another example is the one with disulfide linkages attached to the main epoxy chains.[262] The facile degradation was possible via disulfide exchange reactions thanks to the ability of disulfide bridges to be fragmented and detached from the main epoxy chains.

In the past two decades, many efforts have been made to produce recyclable, reprocessable, and healable epoxies by introducing reversible bonds into the network structure including reversible covalent bonds.[263,264] From such a background, a new class of polymers, known as vitrimers,

was introduced by Leibler et al.[265] Vitrimers are materials containing a cross-linked network with dynamic covalent bonds, where cross-linking density remains unchanged when an exchangeable reaction happens. At a service temperature, vitrimers behave like a traditional thermoset. Once they are heated up to a temperature above the topology freezing transition temperature, an exchangeable reaction occurs rapidly, resulting in a fluid behavior.[265,266] Such a feature makes it possible for the vitrimers to be reprocessed, reshaped, remolded, and recycled.[267]

In most cases, pure epoxy vitrimers seem to not satisfy increasing various industrial demands. Recently, to overcome this, the incorporation of fillers into the vitrimers was proposed. This approach often can provide vitrimer composites with various functions including mechanical reinforcement, stress relaxation, welding, self-healing (repairing) and shape memory.[268] For example, the modulus, yield stress, fracture strain of the epoxy vitrimers could be enhanced by embedding graphene in it. In addition, the shape of the vitrimer could be controlled by near-infrared light due to the photothermal effect of graphene.[269] Also, the photothermal effect of carbon nanotubes (CNT) dispersed in an epoxy vitrimer made it possible to control the welding behavior.[270] Here, it should be noted that for the most vitrimer composites, there exists an inevitable drawback that the stress relaxation is suppressed at the filler interface due to hindered exchangeable reactions because of the less chain mobility.[268] This issue would become more important for the future practical applications.

5.2. Thermal Conductive Materials

Epoxy resins have also been used as electrical insulating materials in electronic components. In recent years, power electronics products have improved greatly in performance and compactness, though the heat generated from the inside has increased along with the improvements. For this reason, how efficiently heat is dissipated to the outside of a device is an important issue that determines the performance and the life of the device, and heat dissipation technology is an extremely important factor. Silica (SiO_2) and alumina (Al_2O_3) particles have been blended as a heat conductive filler to improve the thermal conductivity of an epoxy resin.[271,272] Although the higher filling rate of particles increases the thermal conductivity, the material properties can deteriorate markedly due to the generation of voids. In order to further improve the thermal conductivity, high thermal conductivity fillers such as boron nitride (BN), aluminum nitride (AlN), and silicon carbide (SiC) whisker and their composite systems have been intensively studied.[273−275] However, when the filler content becomes high, it is inevitable that the material properties including processability are negatively affected. Thus, improvements in the thermal conductivity of the epoxy resin itself are keenly sought.

A strategy for increasing the thermal conductivity of an epoxy resin itself is to use the phonon transport mechanism, namely, to realize a highly oriented structure such as a crystalline or liquid crystal polymer. Considering the minimum thermal conductivity model (MTCM)[276] in which the crystalline phase has a higher thermal conductivity, polymers with crystalline domains can be a candidate for a higher thermal conductive material.[277] Similarly, much attention has been focused on emerging highly oriented structures and thereby increasing thermal conductivity by introducing mesogenic groups into the epoxy resins.[278] Lv et al. succeeded in achieving thermal conductivity 2.5 times higher than that of the conventional epoxy resins by using a diamine with an anthraquinone backbone as a curing agent.[279] They employed four isomers with different positions of the amino groups, and demonstrated that all products formed semicrystalline domains and their thermal conductivity had a positive correlation with the mass density. Mo et al. achieved high thermal conductivity by forming an oriented nanostructure and enhancing the chain rigidity when using epoxy mixed with 4,4′-dihydroxydiphenyl (DHDP) in DGEBF.[280] Song et al. also reported high thermal conductivity of an epoxy resin obtained with mesogenic groups.[281] The conductivity was associated with the presence of an agglomerated spherulite structure of highly ordered lamellae. In fact, the thermal conductivity was linearly proportional to the spherulite size, which was determined by the competition between the curing reaction and the spherulite formation. Instead of the self-organization of the highly ordered structure, methods using an external field have also been demonstrated. Harada et al. obtained high thermal conductivity by curing diglycidyl ether terephthalylidene-bis(4-amino-3-methylphenol) (DGETAM) and 4,4′-diaminodiphenylethane (DDE) under a magnetic field, which induces the orientation of mesogenic groups.[282] Although solid strategies are being established for improving thermal conductivity of the epoxy resins, as mentioned above, the next challenge is to achieve a packaging structure for power modules that reduces stress and suppresses void formation.

5.3. Electrically Conductive Materials

Electrically conductive adhesives (ECAs) are promising materials in electronic applications thanks to their lower temperature processability, environmental friendliness (lead-free), and flexibility. Among them, epoxy resins in which silver (Ag) and gold (Au) fillers and carbon-based fillers such as CNT and carbon black (CB) are dispersed are widely used.[211,214,283,284] The main mechanism of the electric conductivity for ECAs is the contact between fillers. Thus, it is necessary to disperse fillers at a high concentration above the percolation threshold.[285] ECAs are classified into two types: isotropic conductive adhesives (ICAs) and anisotropic conductive adhesives (ACAs).[286,287] In ICAs, the electric current flows in all directions, while in ACAs it flows in only one direction. This depends on whether the morphology formed by the filler is isotropic or anisotropic. ICAs are used as an alternative to solder in heat-sensitive electronic components. Among metal fillers, Ag is often used because of its high conductivity and corrosion resistance.[288] Wu et al. reported on epoxy-based ICA filled with Ag nanowires.[289] They claimed that their ICA exhibited lower bulk resistivity and higher shear strength with a lower filler content than conventional ICAs filled with micrometer- and nanometer-sized Ag particles. On the other hand, ACAs are widely used in flat panel display modules and flip-chip on glass, etc. In this case, the filler forms a percolated structure along only one direction. Jiang et al. reported high-performance electronic interconnection with CNTs.[290] Also, Massoumi et al. proposed the fabrication procedure for electrically conductive nanocomposite adhesives based on an epoxy resin containing surface-modified multi-walled carbon nanotubes (MWCNTs).[291] The main drawback of these electrically conductive materials can be the high filler loading amount to achieve the desired conductivity, resulting in reduced mechanical properties. To overcome this, the effect

https://doi.org/10.1021/jacsau.2c00120
JACS Au 2022, 2, 1522−1542

of conductive fillers on the curing process is necessary to be better understood.

5.4. Biobased Materials

The global trends toward the principles of sustainable development urge industry to produce renewable and recyclable products synthesized from biobased materials. Figure 24 shows examples of biobased epoxy compounds synthesized from biobased resources such as rosin, sugar, itaconic acid, cardanol, lignin, tannin, and vegetable oil.[292,293] To achieve fully biobased epoxy resins, curing agents were also derived from renewable materials such as modified plant oil, biobased acid and anhydride, amidoamine from rosin and tung oil, lignin, biobased phenol, and rosin acid.[294,295] Although various types of biobased epoxy compounds and curing agents have been hitherto proposed, most of them have not reached commercial products. The major reason for this is the additional cost due to the isolation and synthesis of the natual monomers as with other excellent materials.[295] Thus, the biobased epoxy resins must provide added value to justify their cost. Recently, to this end, various attempts to improve their performance have been ongoing. A typical example for such trials is the preparation of biobased epoxy composites reinforced with nanocellulose (NC), which is a class of shape-anisotropic materials and is generally extracted from natural resources (e.g., wood pulp, cotton, etc.).[126] Utilization of NC as a filler provided fully biobased epoxy composites with the enhanced mechanical and thermal properties.[296,297]

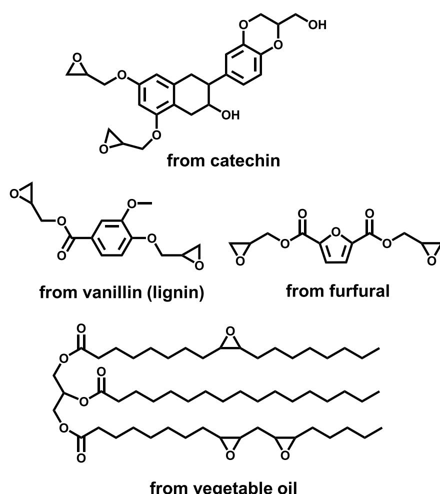

Figure 24. Examples of biobased epoxy compounds synthesized from renewable resources.

6. SUMMARY

Epoxy resins will continue to be in the forefront of many thermoset applications due to their versatile properties. To expand the future applications of epoxy resins, toughness and flexibility, rapid curing potential, self-healing ability, reprocessability, recyclability, high-temperature stability, and conductivity should be improved. A precise prediction of long-term durability is also of pivotal importance from a practical application perspective. This Perspective summarizes works associated with some of the oldest, newest, and most difficult problems. We believe this contributes to a better understanding of how the network formation accompanying the curing reaction affects the physical properties of the resultant epoxy resin and shows that the use of robust physical chemistry techniques will lead to radical advances in thermosetting polymers, with many practical applications.

AUTHOR INFORMATION

Corresponding Authors

Atsuomi Shundo − *Department of Applied Chemistry, Kyushu University, Nishi-ku, Fukuoka 819-0395, Japan;* orcid.org/0000-0002-7898-3233; Email: a-shundo@cstf.kyushu-u.ac.jp

Keiji Tanaka − *Department of Applied Chemistry and Center for Polymer Interface and Molecular Adhesion Science, Kyushu University, Nishi-ku, Fukuoka 819-0395, Japan;* orcid.org/0000-0003-0314-3843; Email: k-tanaka@cstf.kyushu-u.ac.jp

Author

Satoru Yamamoto − *Center for Polymer Interface and Molecular Adhesion Science, Kyushu University, Nishi-ku, Fukuoka 819-0395, Japan;* orcid.org/0000-0002-0238-3039

Complete contact information is available at: https://pubs.acs.org/10.1021/jacsau.2c00120

Notes

The authors declare no competing financial interest.

ACKNOWLEDGMENTS

The authors thank Dr. Mika Aoki for her fruitful discussion and are grateful for support from the JST-Mirai Program (JPMJMI18A2) (K.T.) and the JSPS KAKENHI for Scientific Research (B) (no. JP20H02790, K.T.; no. JP19H02780, A.S.).

REFERENCES

(1) Baekeland, L. H. The Synthesis, Constitution, and Uses of Bakelite. *J. Ind. Eng. Chem.* **1909**, *1* (3), 149−161.
(2) Pascault, J.-P.; Sautereau, H.; Verdu, J.; Williams, R. J. J. In *Thermosetting Polymers*, 1st ed.; CRC Press, 2002; pp1−5.
(3) Kandelbauer, A. Processing. In *Handbook of Thermoset Plastics*, 3rd ed.; Dodiuk, H., Goodman, S. H., Eds.; William Andrew, 2014; pp739−753.
(4) Prolongo, S. G.; del Rosario, G.; Urena, A. Comparative Study on the Adhesive Properties of Different Epoxy Resins. *Int. J. Adhes. Adhes.* **2006**, *26* (3), 125−132.
(5) Liu, Y. Trends of Power Semiconductor Wafer Level Packaging. *Microelectron. Reliab.* **2010**, *50* (4), 514−521.
(6) Yousefi, N.; Sun, X. Y.; Lin, X. Y.; Shen, X.; Jia, J. J.; Zhang, B.; Tang, B. Z.; Chan, M. S.; Kim, J. K. Highly Aligned Graphene/Polymer Nanocomposites with Excellent Dielectric Properties for High-performance Electromagnetic Interference Shielding. *Adv. Mater.* **2014**, *26* (31), 5480−5487.
(7) Forsdyke, K. l.; Starr, T. F. *Thermoset Resins Market Report*; Smithers Rapra Technology, 2002; pp53−57.
(8) Ratna, D. *Handbook of Thermoset Resins*; Smithers Rapra Technology, 2009; pp155−181.
(9) Vidil, T.; Tournilhac, F.; Musso, S.; Robisson, A.; Leibler, L. Control of Reactions and Network Structures of Epoxy Thermosets. *Prog. Polym. Sci.* **2016**, *62*, 126−179.
(10) Xiang, Q.; Xiao, F. P. Applications of Epoxy Materials in Pavement Engineering. *Constr. Build. Mater.* **2020**, *235*, 117529.
(11) Dearborn, E. C.; Fuoss, R. M.; MacKenzie, A. K.; Shepherd, R. G. Epoxy Resins from Bis-, Tris-, and Tetrakisglycidyl Ethers. *Ind. Eng. Chem.* **1953**, *45* (12), 2715−2721.

(12) Pearce, P. J.; Davidson, R. G.; Morris, C. E. M. Hydrolytic Stability of Some Uncured Epoxy Resins. *J. Appl. Polym. Sci.* **1981**, *26* (7), 2363−2372.
(13) Tanaka, K.; Yamaguchi, M. Dynamic-mechanical Properties of Multifunctional Epoxy Resin Cured with Diamine and Filled with Pitch-based Carbon Short Fibers Treated with Coupling Agents. *Adv. Compos. Mater.* **1995**, *5* (1), 45−62.
(14) Mustata, F.; Bicu, I. Multifunctional Epoxy Resins: Synthesis and Characterization. *J. Appl. Polym. Sci.* **2000**, *77* (11), 2430−2436.
(15) Fache, M.; Monteremal, C.; Boutevin, B.; Caillol, S. Amine Hardeners and Epoxy Cross-linker from Aromatic Renewable Resources. *Eur. Polym. J.* **2015**, *73*, 344−362.
(16) Chiao, L. Mechanistic Reaction-kinetics of 4,4'-Diaminodiphenyl Sulfone Cured Tetraglycidyl-4,4'-diaminodiphenylmethane Epoxy-resins. *Macromolecules* **1990**, *23* (5), 1286−1290.
(17) Hsieh, T. H.; Su, A. C. Cure Kinetics of an Epoxy-novolac Molding Compound. *J. Appl. Polym. Sci.* **1990**, *41* (5−6), 1271−1280.
(18) Rwei, S. P.; Liu, A. Y.; Liou, G. S.; Cheng, K. C.; Guo, W. Curing and Pyrolysis of Cresol Novolac Epoxy Resins Containing 2-(6-Oxido-6H-dibenz (c,e) (1,2)oxaphosphorin-6-yl)-1,4-naphthalenediol. *Polym. Eng. Sci.* **2004**, *44* (2), 376−387.
(19) Wu, S.; Soucek, M. D. Crosslinking of Acrylic Latex Coatings with Cycloaliphatic Diepoxide. *Polymer* **2000**, *41* (6), 2017−2028.
(20) Lu, M. P.; Liu, Y. C.; Du, X. X.; Zhang, S. H.; Chen, G. K.; Zhang, Q.; Yao, S.; Liang, L. Y.; Lu, M. G. Cure Kinetics and Properties of High Performance Cycloaliphatic Epoxy Resins Cured with Anhydride. *Ind. Eng. Chem. Res.* **2019**, *58* (16), 6907−6918.
(21) Morita, Y. Cationic Polymerization of Hydrogenated Bisphenol-A Glycidyl Ether with Cycloaliphatic Epoxy Resin and Its Thermal Discoloration. *J. Appl. Polym. Sci.* **2005**, *97* (3), 1395−1400.
(22) Spurr, A. R. A Low-viscosity Epoxy Resin Embedding Medium for Electron Microscopy. *J. Ultrastruct. Res.* **1969**, *26* (1−2), 31−43.
(23) Liu, W. S.; Wang, Z. G.; Xiong, L.; Zhao, L. N. Phosphorus-containing Liquid Cycloaliphatic Epoxy Resins for Reworkable Environment-friendly Electronic Packaging Materials. *Polymer* **2010**, *51* (21), 4776−4783.
(24) Katritzky, A. R.; Ramsden. C, A.; Joule, J. A.; Zhdankin, V. V. Structure of Small and Large Rings. In *Handbook of Heterocyclic Chemistry*, 3rd ed; Elsevier, 2010; pp 210−237.
(25) Ellis, B. Introduction to the Chemistry, Synthesis, Manufacture and Characterization of Epoxy Resins. In *Chemistry and Technology of Epoxy Resins*; Springer, 1993; pp 1−36.
(26) Jin, F. L.; Li, X.; Park, S. J. Synthesis and Application of Epoxy Resins: A Review. *J. Ind. Eng. Chem.* **2015**, *29*, 1−11.
(27) Bouillon, N.; Pascault, J. P.; Tighzert, L. Epoxy Prepolymers Cured with Boron Trifluoride-amine Complexes, 2. Polymerization Mechanisms. *Makromol. Chem.* **1990**, *191* (6), 1417−1433.
(28) Ghaemy, M. The Polymerization Mechanism and Kinetics of DGEBA with BF_3-EDA. *Eur. Polym. J.* **1998**, *34* (8), 1151−1156.
(29) Crivello, J. V.; Lam, J. H. W. Diaryliodonium Salts - New Class of Photo-initiators for Cationic Polymerization. *Macromolecules* **1977**, *10* (6), 1307−1315.
(30) Crivello, J. V.; Lam, J. H. W. Photoinitiated Cationic Polymerization with Triarylsulfonium Salts. *J. Polym. Sci. A Polym. Chem.* **1979**, *17* (4), 977−999.
(31) Takuma, K.; Takata, T.; Endo, T. Cationic Polymerization of Epoxide with Benzyl Phosphonium Salts as the Latent Thermal Initiator. *Macromolecules* **1993**, *26* (4), 862−863.
(32) Yagci, Y.; Reetz, I. Externally Stimulated Initiator Systems for Cationic Polymerization. *Prog. Polym. Sci.* **1998**, *23* (8), 1485−1538.
(33) Heise, M. S.; Martin, G. C. Curing Mechanism and Thermal-properties of Epoxy Imidazole Systems. *Macromolecules* **1989**, *22* (1), 99−104.
(34) Jisova, V. Curing Mechanism of Epoxides by Imidazoles. *J. Appl. Polym. Sci.* **1987**, *34* (7), 2547−2558.
(35) Maka, H.; Spychaj, T.; Pilawka, R. Epoxy Resin/Ionic Liquid Systems: The Influence of Imidazolium Cation Size and Anion Type on Reactivity and Thermomechanical Properties. *Ind. Eng. Chem. Res.* **2012**, *51* (14), 5197−5206.
(36) Matejka, L.; Pokorny, S.; Dusek, K. Acid Curing of Epoxy Resins - A Comparison between the Polymerization of Diepoxide-diacid and Monoepoxide-cyclic Anhydride Systems. *Makromol. Chem.* **1985**, *186* (10), 2025−2036.
(37) Rocks, J.; Rintoul, L.; Vohwinkel, F.; George, G. The Kinetics and Mechanism of Cure of an Amino-glycidyl Epoxy Resin by a Co-anhydride as Studied by FT-Raman Spectroscopy. *Polymer* **2004**, *45* (20), 6799−6811.
(38) Fernandez-Francos, X.; Ramis, X.; Serra, A. From Curing Kinetics to Network Structure: A Novel Approach to the Modeling of the Network Buildup of Epoxy-anhydride Thermosets. *J. Polym. Sci. A Polym. Chem.* **2014**, *52* (1), 61−75.
(39) Dusek, K.; Ilavsky, M. Formation, Structure, and Elasticity of Loosely Crosslinked Epoxy-amine Networks, 1. Statistics of Formation. *J. Polym. Sci. B Polym. Phys.* **1983**, *21* (8), 1323−1339.
(40) Galante, M. J.; Williams, R. J. J. Polymer Networks Based on the Diepoxide Diisocyanate Reaction Catalyzed by Tertiary-amines. *J. Appl. Polym. Sci.* **1995**, *55* (1), 89−98.
(41) Yang, J. L.; Keller, M. W.; Moore, J. S.; White, S. R.; Sottos, N. R. Microencapsulation of Isocyanates for Self-healing Polymers. *Macromolecules* **2008**, *41* (24), 9650−9655.
(42) Yuan, Y. C.; Rong, M. Z.; Zhang, M. Q.; Yang, G. C.; Zhao, J. Q. Self-healing of Fatigue Crack in Epoxy Materials with Epoxy/mercaptan System. *Express Polym. Lett.* **2011**, *5* (1), 47−59.
(43) Flores, M.; Fernandez-Francos, X.; Morancho, J. M.; Serra, A.; Ramis, X. Ytterbium Triflate as a New Catalyst on the Curing of Epoxy-isocyanate Based Thermosets. *Thermochim. Acta* **2012**, *543*, 188−196.
(44) Shechter, L.; Wynstra, J.; Kurkjy, R. P. Glycidyl Ether Reactions with Amines. *Ind. Eng. Chem.* **1956**, *48* (1), 94−97.
(45) Mora, A. S.; Tayouo, R.; Boutevin, B.; David, G.; Caillol, S. A Perspective Approach on the Amine Reactivity and the Hydrogen Bonds Effect on Epoxy-amine Systems. *Eur. Polym. J.* **2020**, *123*, 109460.
(46) Thomas, R.; Durix, S.; Sinturel, C.; Omonov, T.; Goossens, S.; Groeninckx, G.; Moldenaers, P.; Thomas, S. Cure Kinetics, Morphology and Miscibility of Modified DGEBA-based Epoxy Resin - Effects of a Liquid Rubber Inclusion. *Polymer* **2007**, *48* (6), 1695−1710.
(47) Duemichen, E.; Javdanitehran, M.; Erdmann, M.; Trappe, V.; Sturm, H.; Braun, U.; Ziegmann, G. Analyzing the Network Formation and Curing Kinetics of Epoxy Resins by in Situ Near-infrared Measurements with Variable Heating Rates. *Thermochim. Acta* **2015**, *616*, 49−60.
(48) Gilbert, M. D.; Schneider, N. S.; MacKnight, W. J. Mechanism of the Dicyandiamide Epoxide Reaction. *Macromolecules* **1991**, *24* (2), 360−369.
(49) Raetzke, K.; Shaikh, M. Q.; Faupel, F.; Noeske, P. L. M. Shelf Stability of Reactive Adhesive Formulations: A Case Study for Dicyandiamide-cured Epoxy Systems. *Int. J. Adhes. Adhes.* **2010**, *30* (2), 105−110.
(50) Lin, Y. G.; Sautereau, H.; Pascault, J. P. Processing Property Relationship for Dicyandiamide-cured Epoxy Networks. *J. Appl. Polym. Sci.* **1987**, *33* (2), 685−691.
(51) Tomuta, A. M.; Ramis, X.; Ferrando, F.; Serra, A. The Use of Dihydrazides as Latent Curing Agents in Diglycidyl Ether of Bisphenol A Coatings. *Prog. Org. Coat.* **2012**, *74* (1), 59−66.
(52) Spindler, R.; Fréchet, J. M. J. Synthesis and Characterization of Hyperbranched Polyurethanes Prepared from Blocked Isocyanate Monomers by Step-growth Polymerization. *Macromolecules* **1993**, *26* (18), 4809−4813.
(53) Wicks, D. A.; Wicks, Z. W. Blocked Isocyanates III Part B: Uses and Applications of Blocked Isocyanates. *Prog. Org. Coat.* **2001**, *41* (1−3), 1−83.
(54) Suzuki, K.; Nobuki, M.; Horii, H.; Sugita, Y.; Sanda, F.; Endo, T. One-pot Curing System of Epoxy Resin Imines Initiated with Water. *J. Appl. Polym. Sci.* **2003**, *88* (4), 878−882.

https://doi.org/10.1021/jacsau.2c00120
JACS Au 2022, 2, 1522−1542

(55) Suzuki, K.; Matsu-ura, N.; Horii, H.; Sugita, Y.; Sanda, F.; Endo, T. Diethyl Ketone-based Imine as Efficient Latent Hardener for Epoxy Resin. *J. Appl. Polym. Sci.* **2002**, *83* (8), 1744−1749.

(56) Okuhira, H.; Kii, T.; Ochi, M.; Takeyama, H. Novel Moisture-curable Epoxy Resins and Their Characterization. *J. Appl. Polym. Sci.* **2003**, *89* (1), 91−95.

(57) Cameron, J. F.; Fréchet, J. M. J. Photogeneration of Organic-bases from Ortho-nitrobenzyl-derived Carbamates. *J. Am. Chem. Soc.* **1991**, *113* (11), 4303−4313.

(58) Arimitsu, K.; Miyamoto, M.; Ichimura, K. Applications of A Nonlinear Organic Reaction of Carbamates to Proliferate Aliphatic Amines. *Angew. Chem., Int. Ed.* **2000**, *39* (19), 3425−3428.

(59) Ito, K. I.; Nishimura, M.; Sashio, M.; Tsunooka, M. Thermal Cross-linking of Poly(glycidyl methacrylate) films and Epoxy Resin Films Using Amines Formed by Photolysis of *O*-Acyloximes. *J. Polym. Sci. A Polym. Chem.* **1994**, *32* (9), 1793−1796.

(60) Liu, X. D.; Kimura, M.; Sudo, A.; Endo, T. Accelerating Effects of *N*-Aryl-*N* ', *N* '-dialkyl Ureas on Epoxy-dicyandiamide Curing System. *J. Polym. Sci. A Polym. Chem.* **2010**, *48* (23), 5298−5305.

(61) Unruh, D. A.; Pastine, S. J.; Moreton, J. C.; Frechet, J. M. J. Thermally Activated, Single Component Epoxy Systems. *Macromolecules* **2011**, *44* (16), 6318−6325.

(62) Gupta, A. M.; Macosko, C. W. Modeling Strategy for Systems with Both Stepwise and Chainwise Chemistry - Amine-epoxy Networks with Etherification. *J. Polym. Sci. B Polym. Phys.* **1990**, *28* (13), 2585−2606.

(63) Cizmecioglu, M.; Gupta, A.; Fedors, R. F. Influence of Cure Conditions on Glass-transition Temperature and Density of an Epoxy Resin. *J. Appl. Polym. Sci.* **1986**, *32* (8), 6177−6190.

(64) Montserrat, S. Vitrification and Further Structural Relaxation in the Isothermal Curing of an Epoxy Resin. *J. Appl. Polym. Sci.* **1992**, *44* (3), 545−554.

(65) Rabinowitch, E. Collision, Co-ordination, Diffusion and Reaction Velocity in Condensed Systems. *Trans. Faraday Soc.* **1937**, *33* (2), 1225−1232.

(66) Wise, C. W.; Cook, W. D.; Goodwin, A. A. Chemico-diffusion Kinetics of Model Epoxy-amine Resins. *Polymer* **1997**, *38* (13), 3251−3261.

(67) Mak, H. D.; Rogers, M. G. Determination of Chain Branching in Epoxy Resins by Nuclear Magnetic Resonance Spectrometry. *Anal. Chem.* **1972**, *44* (4), 837−839.

(68) Cocker, R. P.; Chadwick, D. L.; Dare, D. J.; Challis, R. E. A Low Resolution Pulsed NMR and Ultrasound Study to Monitor the Cure of an Epoxy Resin Adhesive. *Int. J. Adhes. Adhes.* **1998**, *18* (5), 319−331.

(69) Podzimek, S.; Kastanek, A. Characterization of Bisphenol A-based Epoxy Resins by HPLC, GPC, GPC-MALLS, VPO, Viscometry, and End Group Analysis: On the Identification of 2,3-Dihydroxypropyl-containing Compounds, Determination of Molar Mass Distribution, and Branching. *J. Appl. Polym. Sci.* **1999**, *74* (10), 2432−2438.

(70) Chian, W.; Timm, D. C. Kinetic Reaction Analysis of an Anhydride-cured Thermoplastic Epoxy: PGE/NMA/BDMA. *Macromolecules* **2004**, *37* (21), 8091−8097.

(71) Riccardi, C. C.; Adabbo, H. E.; Williams, R. J. J. Curing Reaction of Epoxy Resins with Diamines. *J. Appl. Polym. Sci.* **1984**, *29* (8), 2481−2492.

(72) Javdanitehran, M.; Berg, D. C.; Duemichen, E.; Ziegmann, G. An Iterative Approach for Isothermal Curing Kinetics Modelling of an Epoxy Resin System. *Thermochim. Acta* **2016**, *623*, 72−79.

(73) Zvetkov, V. L.; Calado, V. Comparative DSC Kinetics of the Reaction of DGEBA with Aromatic Diamines. III. Formal Kinetic Study of the Reaction of DGEBA with Diamino Diphenyl Methane. *Thermochim. Acta* **2013**, *560*, 95−103.

(74) Moroni, A.; Mijovic, J.; Pearce, E. M.; Foun, C. C. Cure Kinetics of Epoxy Resins and Aromatic Diamines. *J. Appl. Polym. Sci.* **1986**, *32* (2), 3761−3773.

(75) Chabert, B.; Lachenal, G.; Tung, C. V. Epoxy Resins and Epoxy Blends Studied by Near-infrared Spectroscopy. *Macromolecul. Symp.* **1995**, *94* (1), 145−158.

(76) Gonzalez, M. G.; Cabanelas, J. C.; Baselga, J. Applications of FTIR on Epoxy Resins - Identification, Monitoring the Curing Process, Phase Separation and Water Uptake. In *Infrared Spectroscopy - Materials Science, Engineering and Technology*; Theophanides, T., Eds.; InTech, 2012; pp 261−284.

(77) Huang, C. Y.; Sun, X. T.; Yuan, H. F.; Song, C. F.; Meng, Y.; Li, X. Y. Study on the Reactivity and Kinetics of Primary and Secondary Amines During Epoxy Curing by NIR Spectroscopy Combined with Multivariate Analysis. *Vib. Spectrosc.* **2020**, *106*, 102993.

(78) Pandita, S. D.; Wang, L. W.; Mahendran, R. S.; Machavaram, V. R.; Irfan, M. S.; Harris, D.; Fernando, G. F. Simultaneous DSC-FTIR Spectroscopy: Comparison of Cross-linking Kinetics of an Epoxy/amine Resin System. *Thermochim. Acta* **2012**, *543* (10), 9−17.

(79) Sbirrazzuoli, N.; Mititelu-Mija, A.; Vincent, L.; Alzina, C. Isoconversional Kinetic Analysis of Stoichiometric and Off-stoichiometric Epoxy-amine Cures. *Thermochim. Acta* **2006**, *447* (2), 167−177.

(80) Sourour, S.; Kamal, M. R. Differential Scanning Calorimetry of Epoxy Cure - Isothermal Cure Kinetics. *Thermochim. Acta* **1976**, *14* (1−2), 41−59.

(81) Zvetkov, V. L.; Krastev, R. K.; Paz-Abuin, S. Is the Kamal's Model Appropriate in the Study of the Epoxy-amine Addition Kinetics? *Thermochim. Acta* **2010**, *505* (1−2), 47−52.

(82) Dušek, K.; Havlíček, I. Diffusion-controlled Kinetics of Cross-linking. *Prog. Org. Coat.* **1993**, *22* (1−4), 145−159.

(83) Chern, C. S.; Poehlein, G. W. A Kinetic-model for Curing Reactions of Epoxides with Amines. *Polym. Eng. Sci.* **1987**, *27* (11), 788−795.

(84) Wisanrakkit, G.; Gillham, J. K. The Glass-transition Temperature (T_g) as an Index of Chemical Conversion for a High-Tg Amine Epoxy System - Chemical and Diffusion-controlled Reaction-kinetics. *J. Appl. Polym. Sci.* **1990**, *41* (11−12), 2885−2929.

(85) Charlesworth, J. Analysis of the Substitution Effects Involved in Diepoxide-diamine Copolymerization Reactions. *J. Polym. Sci. A Polym. Chem.* **1980**, *18* (2), 621−628.

(86) Mijovic, J.; Fishbain, A.; Wijaya, J. Mechanistic Modeling of Epoxy Amine Kinetics, 1. Model-compound Study. *Macromolecules* **1992**, *25* (2), 979−985.

(87) Stjohn, N. A.; George, G. A. Cure Kinetics and Mechanisms of A Tetraglycidyl-4,4'-diaminodiphenylmethane Diaminodiphenylsulphone Epoxy Resin Using Near IR Spectroscopy. *Polymer* **1992**, *33* (13), 2679−2688.

(88) Aoki, M.; Shundo, A.; Yamamoto, S.; Tanaka, K. Effect of A Heterogeneous Network on Glass Transition Dynamics and Solvent Crack Behavior of Epoxy Resins. *Soft Matter* **2020**, *16* (32), 7470−7478.

(89) PazAbuin, S.; Pellin, M. P.; PazPazos, M.; LopezQuintela, A. Influence of the Reactivity of Amine Hydrogens and the Evaporation of Monomers on the Cure Kinetics of Epoxy-amine: Kinetic Questions. *Polymer* **1997**, *38* (15), 3795−3804.

(90) Sahagun, C. M.; Morgan, S. E. Thermal Control of Nanostructure and Molecular Network Development in Epoxy-amine Thermosets. *ACS Appl. Mater. Interfaces* **2012**, *4* (2), 564−572.

(91) Dušek, K.; Pleštil, J.; Lednický, F.; Luňák, S. Are Cured Epoxy Resins Inhomogeneous. *Polymer* **1978**, *19* (4), 393−397.

(92) Mijovic, J.; Koutsky, J. A. Correlation between Nodular Morphology and Fracture Properties of Cured Epoxy Resins. *Polymer* **1979**, *20* (9), 1095−1107.

(93) Takahama, T.; Geil, P. H. Structural Inhomogeneities of Cured Epoxy Resins. *Makromol. Chem. Rapid Commun.* **1982**, *3* (6), 389−394.

(94) Gupta, V. B.; Drzal, L. T.; Adams, W. W.; Omlor, R. An Electron-microscopic Study of the Morphology of Cured Epoxy resin. *J. Mater. Sci.* **1985**, *20* (10), 3439−3452.

(95) Sahagun, C. M.; Knauer, K. M.; Morgan, S. E. Molecular Network Development and Evolution of Nanoscale Morphology in an

Epoxy-amine Thermoset Polymer. *J. Appl. Polym. Sci.* **2012**, *126* (4), 1394−1405.
(96) Haba, D.; Kaufmann, J.; Brunner, A. J.; Resch, K.; Teichert, C. Observation of Elastic Modulus Inhomogeneities in Thermosetting Epoxies Using AFM - Discerning Facts and Artifacts. *Polymer* **2014**, *55* (16), 4032−4040.
(97) Dazzi, A.; Prater, C. B. AFM-IR: Technology and Applications in Nanoscale Infrared Spectroscopy and Chemical Imaging. *Chem. Rev.* **2017**, *117* (7), 5146−5173.
(98) Morsch, S.; Liu, Y. W.; Lyon, S. B.; Gibbon, S. R. Insights into Epoxy Network Nanostructural Heterogeneity Using AFM-IR. *ACS Appl. Mater. Interfaces* **2016**, *8* (1), 959−966.
(99) Morsch, S.; Liu, Y. W.; Greensmith, P.; Lyon, S. B.; Gibbon, S. R. Molecularly Controlled Epoxy Network Nanostructures. *Polymer* **2017**, *108* (1), 146−153.
(100) Izumi, A.; Nakao, T.; Shibayama, M. Gelation and Cross-link Inhomogeneity of Phenolic Resins Studied by ^{13}C-NMR Spectroscopy and Small-angle X-ray Scattering. *Soft Matter* **2013**, *9* (16), 4188−4197.
(101) Shudo, Y.; Izumi, A.; Takeuchi, T.; Nakao, T.; Shibayama, M. Dynamic Light Scattering Study of the Curing Mechanisms of Novolac-type Phenolic Resins. *Polym. J.* **2015**, *47* (6), 428−433.
(102) Izumi, A.; Shudo, Y.; Nakao, T.; Shibayama, M. Cross-link Inhomogeneity in Phenolic Resins at the Initial Stage of Curing Studied by ^{1}H-Pulse NMR Spectroscopy and Complementary SAXS/WAXS and SANS/WANS with a Solvent-swelling Technique. *Polymer* **2016**, *103* (10), 152−162.
(103) Izumi, A.; Nakao, T.; Shibayama, M. Gelation and Cross-link Inhomogeneity of Phenolic Resins Studied by Small- and Wide-angle X-ray Scattering and ^{1}H-Pulse NMR Spectroscopy. *Polymer* **2015**, *59* (2), 226−233.
(104) Aoki, M.; Shundo, A.; Kuwahara, R.; Yamamoto, S.; Tanaka, K. Mesoscopic Heterogeneity in the Curing Process of an Epoxy-amine System. *Macromolecules* **2019**, *52* (5), 2075−2082.
(105) Enns, J. B.; Gillham, J. K. Time Temperature Transformation (TTT) Cure Diagram - Modeling the Cure Behavior of Thermosets. *J. Appl. Polym. Sci.* **1983**, *28* (8), 2567−2591.
(106) Zhang, C.; Wang, Y. C.; Liu, Y. H. Construction of Improved Isothermal TTT Cure Diagram Based on an Epoxy-amine Thermoset. *J. Appl. Polym. Sci.* **2019**, *136* (13), 47279.
(107) Mangialetto, J.; Verhelle, R.; Van Assche, G.; Van den Brande, N.; Van Mele, B. Time-temperature-transformation, Temperature-conversion-transformation, and Continuous-heating-transformation Diagrams of Reversible Covalent Polymer Networks. *Macromolecules* **2021**, *54* (1), 412−425.
(108) Chen, Y. C.; Chiu, W. Y. The Structural Properties of Imidazole Cured Epoxy-phenol Resins. *Polymer* **2001**, *42* (12), 5439−5448.
(109) Chiou, P. L.; Letton, A. Modeling the Chemorheology of an Epoxy Resin System Exhibiting Complex Curing Behavior. *Polymer* **1992**, *33* (18), 3925−3931.
(110) Winter, H. H. Can the Gel Point of a Cross-linking Polymer Be Detected by the *G*'-*G*'' Crossover. *Polym. Eng. Sci.* **1987**, *27* (22), 1698−1702.
(111) Halley, P. J.; Mackay, M. E. Chemorheology of Thermosets - An Overview. *Polym. Eng. Sci.* **1996**, *36* (5), 593−609.
(112) Mortimer, S.; Ryan, A. J.; Stanford, J. L. Rheological Behavior and Gel-point Determination for A Model Lewis Acid-initiated Chain Growth Epoxy Resin. *Macromolecules* **2001**, *34* (9), 2973−2980.
(113) ASTM International. *Standard Test Method for Gel Time and Peak Exothermic Temperature of Reacting Thermosetting Resins*; ASTM D2471-99; West Conshohocken, PA, 1999.
(114) Tung, C. Y. M.; Dynes, P. J. Relationship between Viscoelastic Properties and Gelation in Thermosetting Systems. *J. Appl. Polym. Sci.* **1982**, *27* (2), 569−574.
(115) Matejka, L. Rheology of Epoxy Networks Near the Gel Point. *Polym. Bull.* **1991**, *26* (1), 109−116.
(116) Lairez, D.; Adam, M.; Emery, J. R.; Durand, D. Rheological Behavior of an Epoxy Amine System Near the Gel Point. *Macromolecules* **1992**, *25* (1), 286−289.
(117) Eloundou, J. P.; Gerard, J. F.; Harran, D.; Pascault, J. P. Temperature Dependence of the Behavior of a Reactive Epoxy-amine System by Means of Dynamic Rheology, 2. High-T_g Epoxy-amine System. *Macromolecules* **1996**, *29* (21), 6917−6927.
(118) Lange, J.; Altmann, N.; Kelly, C. T.; Halley, P. J. Understanding Vitrification during Cure of Epoxy Resins Using Dynamic Scanning Calorimetry and Rheological Techniques. *Polymer* **2000**, *41* (15), 5949−5955.
(119) Meng, Y.; Simon, S. L. Relation between Mobility Factor and Diffusion Factor for Thermoset Cure. *Thermochim. Acta* **2005**, *437* (1−2), 179−189.
(120) Valentine, M. T.; Kaplan, P. D.; Thota, D.; Crocker, J. C.; Gisler, T.; Prud'homme, R. K.; Beck, M.; Weitz, D. A. Investigating the Microenvironments of Inhomogeneous Soft Materials with Multiple Particle Tracking. *Phys. Rev. E* **2001**, *64* (6), 061506.
(121) Waigh, T. A. Microrheology of Complex Fluids. *Rep. Prog. Phys.* **2005**, *68* (3), 685−742.
(122) Penaloza, D. P.; Hori, K.; Shundo, A.; Tanaka, K. Spatial Heterogeneity in A Lyotropic Liquid Crystal with Hexagonal Phase. *Phys. Chem. Chem. Phys.* **2012**, *14* (15), 5247−5250.
(123) Penaloza, D. P.; Shundo, A.; Matsumoto, K.; Ohno, M.; Miyaji, K.; Goto, M.; Tanaka, K. Spatial Heterogeneity in the Sol-gel Transition of a Supramolecular System. *Soft Matter* **2013**, *9* (21), 5166−5172.
(124) Shundo, A.; Hori, K.; Penaloza, D. P.; Matsumoto, Y.; Okumura, Y.; Kikuchi, H.; Lee, K. E.; Kim, S. O.; Tanaka, K. Hierarchical Spatial Heterogeneity in Liquid Crystals Composed of Graphene Oxides. *Phys. Chem. Chem. Phys.* **2016**, *18* (32), 22399−22406.
(125) Matsumoto, Y.; Shundo, A.; Ohno, M.; Tsuruzoe, N.; Goto, M.; Tanaka, K. Mesoscopic Heterogeneity in Pore Size of Supramolecular Networks. *Langmuir* **2018**, *34* (25), 7503−7508.
(126) Matsumoto, Y.; Shundo, A.; Hayashi, H.; Tsuruzoe, N.; Tanaka, K. Effect of the Heterogeneous Structure on Mechanical Properties for a Nanocellulose-reinforced Polymer Composite. *Macromolecules* **2019**, *52* (21), 8266−8274.
(127) Shundo, A.; Matsumoto, Y.; Hayashi, H.; Tsuruzoe, N.; Matsuno, H.; Tanaka, K. Mesoscopic Heterogeneity in a Nanocellulose-containing Cell Storage Medium. *J. Mater. Chem. B* **2020**, *8* (21), 4570−4574.
(128) Kogo, T.; Shundo, A.; Wang, C.; Tanaka, K. Spatial Heterogeneity Accompanying Gel Formation of Poly(*N*-isopropylacrylamide) Aqueous Solution at a Temperature below Cloud Point. *Macromolecules* **2020**, *53* (24), 10964−10971.
(129) Nguyen, H. K.; Aoki, M.; Liang, X.; Yamamoto, S.; Tanaka, K.; Nakajima, K. Local Mechanical Properties of Heterogeneous Nanostructures Developed in a Cured Epoxy Network: Implications for Innovative Adhesion Technology. *ACS Applied Nano Materials* **2021**, *4* (11), 12188−12196.
(130) Li, C. Y.; Strachan, A. Molecular Scale Simulations on Thermoset Polymers: A Review. *J. Polym. Sci. B Polym. Phys.* **2015**, *53* (2), 103−122.
(131) Lyulin, S. V.; Larin, S. V.; Nazarychev, V. M.; Fal'kovich, S. G.; Kenny, J. M. Multiscale Computer Simulation of Polymer Nanocomposites Based on Thermoplastics. *Polym. Sci. Ser. C* **2016**, *58* (1), 2−15.
(132) Liu, Z.; Li, J. H.; Zhou, C.; Zhu, W. H. A Molecular Dynamics Study on Thermal and Rheological Properties of BNNS-epoxy Nanocomposites. *Int. J. Heat Mass Transfer* **2018**, *126*, 353−362.
(133) Hsissou, R. Review on Epoxy Polymers and Its Composites as A Potential Anticorrosive Coatings for Carbon Steel in 3.5% NaCl Solution: Computational Approaches. *J. Mol. Liq.* **2021**, *336*, 116307.
(134) Yarovsky, I.; Evans, E. Computer Simulation of Structure and Properties of Crosslinked Polymers: Application to Epoxy Resins. *Polymer* **2002**, *43* (3), 963−969.

https://doi.org/10.1021/jacsau.2c00120
JACS Au 2022, 2, 1522−1542

(135) Wu, C. F.; Xu, W. J. Atomistic Molecular Modelling of Crosslinked Epoxy Resin. *Polymer* **2006**, *47* (16), 6004−6009.
(136) Komarov, P. V.; Chiu, Y. T.; Chen, S. M.; Khalatur, P. G.; Reineker, P. Highly Cross-linked Epoxy Resins: An Atomistic Molecular Dynamics Simulation Combined with A Mapping/reverse Mapping Procedure. *Macromolecules* **2007**, *40* (22), 8104−8113.
(137) Varshney, V.; Patnaik, S. S.; Roy, A. K.; Farmer, B. L. A Molecular Dynamics Study of Epoxy-based Networks: Cross-linking Procedure and Prediction of Molecular and Material Properties. *Macromolecules* **2008**, *41* (18), 6837−6842.
(138) Bandyopadhyay, A.; Valavala, P. K.; Clancy, T. C.; Wise, K. E.; Odegard, G. M. Molecular Modeling of Crosslinked Epoxy Polymers: The Effect of Crosslink Density on Thermomechanical Properties. *Polymer* **2011**, *52* (11), 2445−2452.
(139) Heine, D. R.; Grest, G. S.; Lorenz, C. D.; Tsige, M.; Stevens, M. J. Atomistic Simulations of End-linked Poly(dimethylsiloxane) Networks: Structure and Relaxation. *Macromolecules* **2004**, *37* (10), 3857−3864.
(140) Khare, R.; Paulaitis, M. E.; Lustig, S. R. Generation of Glass Structures for Molecular Simulations of Polymers Containing Large Monomer Units - Application to Polystyrene. *Macromolecules* **1993**, *26* (26), 7203−7209.
(141) Lin, P. H.; Khare, R. Molecular Simulation of Cross-linked Epoxy and Epoxy-POSS Nanocomposite. *Macromolecules* **2009**, *42* (12), 4319−4327.
(142) Rappe, A. K.; Goddard, W. A. Charge Equilibration for Molecular-dynamics Simulations. *J. Phys. Chem.* **1991**, *95* (8), 3358−3363.
(143) Li, C. Y.; Strachan, A. Molecular Simulations of Crosslinking Process of Thermosetting Polymers. *Polymer* **2010**, *51* (25), 6058−6070.
(144) Okabe, T.; Takehara, T.; Inose, K.; Hirano, N.; Nishikawa, M.; Uehara, T. Curing Reaction of Epoxy Resin Composed of Mixed Base Resin and Curing Agent: Experiments and Molecular Simulation. *Polymer* **2013**, *54* (17), 4660−4668.
(145) Oya, Y.; Nakazawa, M.; Shirasu, K.; Hino, Y.; Inuyama, K.; Kikugawa, G.; Li, J.; Kuwahara, R.; Kishimoto, N.; Waizumi, H.; Nishikawa, M.; Waas, A.; Odagiri, N.; Koyanagi, A.; Salviato, M.; Okabe, T. Molecular Dynamics Simulation of Cross-linking Processes and Material Properties for Epoxy Resins Using First-principle Calculation Combined with Global Reaction Route Mapping Algorithms. *Chem. Phys. Lett.* **2021**, *762*, 138104.
(146) Yamamoto, S.; Tanaka, K. Molecular Size Effect on Curing Process for Epoxy and Amine Mixture. *Nihon Reoroji Gakkaishi* **2021**, *49* (2), 55−60.
(147) Yamamoto, S.; Kuwahara, R.; Tanaka, K. Dynamic Behaviour of Water Molecules in Heterogeneous Free Space Formed in an Epoxy Resin. *Soft Matter* **2021**, *17* (25), 6073−6080.
(148) Levita, G.; Depetris, S.; Marchetti, A.; Lazzeri, A. Cross-link Density and Fracture-toughness of Epoxy-resins. *J. Mater. Sci.* **1991**, *26* (9), 2348−2352.
(149) Rahul, R.; Kitey, R. Effect of Cross-linking on Dynamic Mechanical and Fracture Behavior of Epoxy Variants. *Compos. B Eng.* **2016**, *85*, 336−342.
(150) Pandini, S.; Bignotti, F.; Baldi, F.; Sartore, L.; Consolati, G.; Panzarasa, G. Thermomechanical and Large Deformation Behaviors of Antiplasticized Epoxy Resins: Effect of Material Formulation and Network Architecture. *Polym. Eng. Sci.* **2017**, *57* (6), 553−565.
(151) Cook, W. D.; Mehrabi, M.; Edward, G. H. Ageing and Yielding in Model Epoxy Thermosets. *Polymer* **1999**, *40* (5), 1209−1218.
(152) Blanco, M.; Corcuera, M. A.; Riccardi, C. C.; Mondragon, I. Mechanistic Kinetic Model of an Epoxy Resin Cured with a Mixture of Amines of Different Functionalities. *Polymer* **2005**, *46* (19), 7989−8000.
(153) Koike, T. Determination of Glass Transition Temperature from Viscosity and Conductivity Measurements for an Epoxy-amine System During Curing. *J. Appl. Polym. Sci.* **1993**, *50* (11), 1943−1950.
(154) Lesser, A. J.; Crawford, E. The Role of Network Architecture on the Glass Transition Temperature of Epoxy Resins. *J. Appl. Polym. Sci.* **1997**, *66* (2), 387−395.
(155) Shundo, A.; Aoki, M.; Yamamoto, S.; Tanaka, K. Cross-linking Effect on Segmental Dynamics of Well-defined Epoxy Resins. *Macromolecules* **2021**, *54* (13), 5950−5956.
(156) Stutz, H.; Illers, K. H.; Mertes, J. A Generalized Theory for the Glass-transition Temperature of Cross-linked and Uncrosslinked Polymers. *J. Polym. Sci., Part B: Polym. Phys.* **1990**, *28* (9), 1483−1498.
(157) Jeffrey, K.; Pethrick, R. A. Influence of Chemical Structure on Free Volume in Epoxy Resins: A Positron Annihilation Study. *Eur. Polym. J.*. **1994**, *30* (2), 153−158.
(158) Goyanes, S.; Salguleiro, W.; Somoza, A.; Ramos, J. A.; Mondragon, I. Direct Relationships between Volume Variations at Macro and Nanoscale in Epoxy Systems. PALS/PVT Measurements. *Polymer* **2004**, *45* (19), 6691−6697.
(159) Xie, Q.; Liang, S. D.; Liu, B. W.; Fu, K. X.; Zhan, Z. Y.; Lu, L.; Yang, X. M.; Lu, F. C.; Huang, Z. Y. Structure, Microparameters and Properties of Crosslinked DGEBA/MTHPA: A Molecular Dynamics Simulation. *AIP Adv.* **2018**, *8*, 075332.
(160) Uedono, A.; Aiko, W.; Yamamoto, T.; Nakamichi, T.; Tanigawa, S. Open Spaces and Molecular Motions of Acrylic Epoxy-based Network Polymers Probed by Positron Annihilation. *J. Polym. Sci., Part B: Polym. Phys.* **1999**, *37* (20), 2875−2880.
(161) Salgueiro, W.; Ramos, J.; Somoza, A.; Goyanes, S.; Mondragon, I. Nanohole Volume Dependence on the Cure Schedule in Epoxy Thermosetting Networks: A PALS Study. *Polymer* **2006**, *47* (14), 5066−5070.
(162) Patil, P. N.; Rath, S. K.; Sharma, S. K.; Sudarshan, K.; Maheshwari, P.; Patri, M.; Praveen, S.; Khandelwal, P.; Pujari, P. K. Free Volumes and Structural Relaxations in Diglycidyl Ether of Bisphenol-A Based Epoxy-polyether Amine Networks. *Soft Matter* **2013**, *9* (13), 3589−3599.
(163) Soles, C. L.; Chang, F. T.; Gidley, D. W.; Yee, A. F. Contributions of the Nanovoid Structure to the Kinetics of Moisture Transport in Epoxy Resins. *J. Polym. Sci., Part B: Polym. Phys.* **2000**, *38* (5), 776−791.
(164) Odegard, G. M.; Bandyopadhyay, A. Physical Aging of Epoxy Polymers and Their Composites. *J. Polym. Sci., Part B: Polym. Phys.* **2011**, *49* (24), 1695−1716.
(165) Jackson, M.; Kaushik, M.; Nazarenko, S.; Ward, S.; Maskell, R.; Wiggins, J. Effect of Free Volume Hole-size on Fluid Ingress of Glassy Epoxy Networks. *Polymer* **2011**, *52* (20), 4528−4535.
(166) Jilani, W.; Mzabi, N.; Fourati, N.; Zerrouki, C.; Gallot-Lavallee, O.; Zerrouki, R.; Guermazi, H. Effects of Curing Agent on Conductivity, Structural and Dielectric Properties of an Epoxy Polymer. *Polymer* **2015**, *79* (11), 73−81.
(167) Garden, L.; Pethrick, R. A. A Dielectric Study of Water Uptake in Epoxy Resin Systems. *J. Appl. Polym. Sci.* **2017**, *134* (16), 44717.
(168) Williams, J. G. Beta-relaxation in Epoxy Resin-based Networks. *J. Appl. Polym. Sci.* **1979**, *23* (12), 3433−3444.
(169) Wang, Y. M.; Chen, S. F.; Chen, X. C.; Lu, Y. F.; Miao, M. H.; Zhang, D. H. Controllability of Epoxy Equivalent Weight and Performance of Hyperbranched Epoxy Resins. *Composites, Part B* **2019**, *160*, 615−625.
(170) Feng, J. M.; Guo, Z. S. Temperature-frequency-dependent Mechanical Properties Model of Epoxy Resin and Its Composites. *Composites, Part B* **2016**, *85*, 161−169.
(171) Heux, L.; Halary, J. L.; Laupretre, F.; Monnerie, L. Dynamic Mechanical and ^{13}C NMR Investigations of Molecular Motions Involved in the Beta Relaxation of Epoxy Networks Based on DGEBA and Aliphatic Amines. *Polymer* **1997**, *38* (8), 1767−1778.
(172) Bershtein, V. A.; Peschanskaya, N. N.; Halary, J. L.; Monnerie, L. The Sub-T_g Relaxations in Pure and Antiplasticized Model Epoxy Networks as Studied by High Resolution Creep Rate Spectroscopy. *Polymer* **1999**, *40* (24), 6687−6698.

https://doi.org/10.1021/jacsau.2c00120
JACS Au 2022, 2, 1522−1542

(173) Garcia, F. G.; Soares, B. G.; Pita, V.; Sanchez, R.; Rieumont, J. Mechanical Properties of Epoxy Networks Based on DGEBA and Aliphatic Amines. *J. Appl. Polym. Sci.* **2007**, *106* (3), 2047−2055.
(174) Cook, W. D.; Mayr, A. E.; Edward, G. H. Yielding Behaviour in Model Epoxy Thermosets - II. Temperature Dependence. *Polymer* **1998**, *39* (16), 3725−3733.
(175) Tcharkhtchi, A.; Trotignon, J. P.; Verdu, J. Yielding and fracture in crosslinked epoxies. *Makromol. Chem. Macromol. Symp.* **1999**, *147*, 221−234.
(176) Angell, C. A. Formation of Glasses from Liquids and Biopolymers. *Science* **1995**, *267* (5206), 1924−1935.
(177) Kanaya, T.; Tsukushi, I.; Kaji, K. Non-Gaussian Parameter and Heterogeneity of Amorphous Polymers. *Prog. Theor. Phys. Suppl.* **1997**, *126* (126), 133−140.
(178) Adam, G.; Gibbs, J. H. On Temperature Dependence of Cooperative Relaxation Properties in Glass-forming Liquids. *J. Chem. Phys.* **1965**, *43* (1), 139−146.
(179) Donth, E. The Size of Cooperatively Rearranging Regions at the Glass Transition. *J. Non-Cryst. Solids* **1982**, *53* (3), 325−330.
(180) Matsuoka, S.; Quan, X. A Model for Intermolecular Cooperativity in Conformational Relaxations Near the Glass-transition. *Macromolecules* **1991**, *24* (10), 2770−2779.
(181) Achibat, T.; Boukenter, A.; Duval, E.; Lorentz, G.; Etienne, S. Low-frequency Raman Scattering and Structure of Amorphous Polymers Stretching Effect. *J. Chem. Phys.* **1991**, *95* (4), 2949−2954.
(182) Hong, L.; Novikov, V. N.; Sokolov, A. P. Is There a Connection between Fragility of Glass Forming Systems and Dynamic Heterogeneity/Cooperativity? *J. Non-Cryst. Solids* **2011**, *357* (2), 351−356.
(183) Fischer, E. W.; Donth, E.; Steffen, W. Temperature Dependence of Characteristic Length for Glass Transition. *Phys. Rev. Lett.* **1992**, *68* (15), 2344−2346.
(184) Hong, L.; Gujrati, P. D.; Novikov, V. N.; Sokolov, A. P. Molecular Cooperativity in the Dynamics of Glass-forming Systems: A New Insight. *J. Chem. Phys.* **2009**, *131* (19), 194511.
(185) Tracht, U.; Wilhelm, M.; Heuer, A.; Feng, H.; Schmidt-Rohr, K.; Spiess, H. W. Length Scale of Dynamic Heterogeneities at the Glass Transition Determined by Multidimensional Nuclear Magnetic Resonance. *Phys. Rev. Lett.* **1998**, *81* (13), 2727−2730.
(186) Qiu, X. H.; Ediger, M. D. Length Scale of Dynamic Heterogeneity in Supercooled D-Sorbitol: Comparison to Model Predictions. *J. Phys. Chem. B* **2003**, *107* (2), 459−464.
(187) Hempel, E.; Hempel, G.; Hensel, A.; Schick, C.; Donth, E. Characteristic Length of Dynamic Glass Transition Near T_g For a Wide Assortment of Glass-forming Substances. *J. Phys. Chem. B* **2000**, *104* (11), 2460−2466.
(188) Rijal, B.; Delbreilh, L.; Saiter, A. Dynamic Heterogeneity and Cooperative Length Scale at Dynamic Glass Transition in Glass Forming Liquids. *Macromolecules* **2015**, *48* (22), 8219−8231.
(189) Jilani, W.; Mzabi, N.; Fourati, N.; Zerrouki, C.; Gallot-Lavallee, O.; Zerrouki, R.; Guermazi, H. A Comparative Study of Structural and Dielectric Properties of Diglycidyl Ether of Bisphenol A (DGEBA) Cured with Aromatic or Aliphatic Hardeners. *J. Mater. Sci.* **2016**, *51* (17), 7874−7886.
(190) Shundo, A.; Aoki, M.; Yamamoto, S.; Tanaka, K. Effect of Cross-linking Density on Horizontal and Vertical Shift Factors in Linear Viscoelastic Functions of Epoxy Resins. *Macromolecules* **2021**, *54* (20), 9618−9624.
(191) Huang, Y.; Kinloch, A. J. The Use of Time-temperature Superpositioning in Studying the Fracture Properties of Rubber-toughened Epoxy Polymers. *J. Adhes.* **1993**, *41* (1−4), 5−22.
(192) Ghosh, S. K.; Rajesh, P.; Srikavya, B.; Rathore, D. K.; Prusty, R. K.; Ray, B. C. Creep Behaviour Prediction of Multi-layer Graphene Embedded Glass Fiber/Epoxy Composites Using Time-temperature Superposition Principle. *Composites, Part A* **2018**, *107*, 507−518.
(193) Anand, A.; Banerjee, P.; Prusty, R. K.; Ray, B. C. Lifetime Prediction of Nano-silica Based Glass Fibre/Epoxy Composite by Time Temperature Superposition Principle. *IOP Conf. Ser.: Mater. Sci. Eng.* **2018**, *338*, 012020.
(194) Pohl, M.; Kupfer, R.; Koch, I.; Modler, N.; Hufenbach, W. A. Determination of the Long-term Properties in Laminate-thickness Direction of Textile-reinforced Thermoplastic Composites under Compression Using Time-temperature Superposition. *Adv. Eng. Mater.* **2016**, *18* (3), 369−375.
(195) Schwarzl, F.; Staverman, A. J. Time-temperature Dependence of Linear Viscoelastic Behavior. *J. Appl. Phys.* **1952**, *23* (8), 838−843.
(196) Tobolsky, A. V. Stress Relaxation Studies of the Viscoelastic Properties of Polymers. *J. Appl. Phys.* **1956**, *27* (7), 673−685.
(197) Kramer, E. J. Molecular Theory of the Fracture-toughness of Low-molecular Weight Polymers. *J. Mater. Sci.* **1979**, *14* (6), 1381−1388.
(198) Kogan, L.; Hui, C. Y.; Ruina, A. Theory of Chain Pull-out and Stability of Weak Polymer Interfaces.1. *Macromolecules* **1996**, *29* (11), 4090−4100.
(199) Sanchez-Valencia, A.; Smerdova, O.; Hutchings, L. R.; De Focatiis, D. S. A. The Roles of Blending and of Molecular Weight Distribution on Craze Initiation. *Macromolecules* **2017**, *50* (23), 9507−9514.
(200) Donald, A. M.; Kramer, E. J. Effect of Molecular Entanglements on Craze Microstructure in Glassy-polymers. *J. Polym. Sci., Part B: Polym. Phys.* **1982**, *20* (5), 899−909.
(201) Liu, J. W.; Yee, A. F. Effect of Local Conformational Transition on Craze Initiation in Polyestercarbonates Containing Cyclohexylene Linkages. *Macromolecules* **2000**, *33* (4), 1338−1344.
(202) Bell, J. P. Mechanical Properties of a Glassy Epoxide Polymer - Effect of Molecular Weight between Crosslinks. *J. Appl. Polym. Sci.* **1970**, *14* (7), 1901−1906.
(203) Cho, K.; Lee, D.; Park, C. E. Effect of Molecular Weight between Crosslinks on Fracture Behaviour of Diallylterephthalate Resins. *Polymer* **1996**, *37* (5), 813−817.
(204) Yamini, S.; Young, R. J. The Mechanical Properties of Epoxy Resins 2. Effect of Plastic Deformation Upon Crack Propagation. *J. Mater. Sci.* **1980**, *15* (7), 1823−1831.
(205) Chuang, Y. F.; Wu, H. C.; Yang, F. Q.; Yang, T. J.; Lee, S. Cracking and Healing in Poly (methyl methacrylate): Effect of Solvent. *J. Polym. Res.* **2016**, *24* (2), 1−11.
(206) Toscano, A.; Pitarresi, G.; Scafidi, M.; Di Filippo, M.; Spadaro, G.; Alessi, S. Water Diffusion and Swelling Stresses in Highly Crosslinked Epoxy Matrices. *Polym. Degrad. Stab.* **2016**, *133*, 255−263.
(207) Yee, A. F.; Pearson, R. A. Toughening Mechanisms in Elastomer-modified Epoxies.1. Mechanical Studies. *J. Mater. Sci.* **1986**, *21* (7), 2462−2474.
(208) Huang, Y.; Kinloch, A. J. The Role of Plastic Void Growth in the Fracture of Rubber-toughened Epoxy Polymers. *J. Mater. Sci. Lett.* **1992**, *11* (8), 484−487.
(209) Azimi, H. R.; Pearson, R. A.; Hertzberg, R. W. Fatigue of Rubber-modified Epoxies: Effect of Particle Size and Volume Fraction. *J. Mater. Sci.* **1996**, *31* (14), 3777−3789.
(210) Hodgkin, J. H.; Simon, G. P.; Varley, R. J. Thermoplastic Toughening of Epoxy Resins: A Critical Review. *Polym. Adv. Technol.* **1998**, *9* (1), 3−10.
(211) Chandrasekaran, V. C. S.; Advani, S. G.; Santare, M. H. Role Of Processing on Interlaminar Shear Strength Enhancement of Epoxy/Glass Fiber/Multi-walled Carbon Nanotube Hybrid Composites. *Carbon* **2010**, *48* (13), 3692−3699.
(212) Zabihi, O.; Ahmadi, M.; Nikafshar, S.; Preyeswary, K. C.; Naebe, M. A Technical Review on Epoxy-clay Nanocomposites: Structure, Properties, and Their Applications in Fiber Reinforced Composites. *Composites, Part B* **2018**, *135*, 1−24.
(213) El-Fattah, M. A.; El Saeed, A. M.; El-Ghazawy, R. A. Chemical Interaction of Different Sized Fumed Silica with Epoxy Via Ultrasonication for Improved Coating. *Prog. Org. Coat.* **2019**, *129*, 1−9.
(214) Sasidharan, S.; Anand, A. Epoxy-based Hybrid Structural Composites with Nanofillers: A Review. *Ind. Eng. Chem. Res.* **2020**, *59* (28), 12617−12631.

(215) Shundo, A.; Sakurai, T.; Takafuji, M.; Nagaoka, S.; Ihara, H. Molecular-length and Chiral Discriminations by β-Structural Poly (L-alanine) on Silica. *J. Chromatogr. A* **2005**, *1073* (1−2), 169−174.
(216) Bagwe, R. P.; Hilliard, L. R.; Tan, W. H. Surface Modification of Silica Nanoparticles to Reduce Aggregation and Nonspecific Binding. *Langmuir* **2006**, *22* (9), 4357−4362.
(217) Shundo, A.; Mallik, A. K.; Nakashima, H.; Takafuji, M.; Nagaoka, S.; Chowdhury, M. A. J.; Ihara, H. Enhancement of Discrimination Ability for Cis- and Trans-decalins through Side-chain Ordering in Comb-shaped Polymer. *Chem. Lett.* **2010**, *39* (8), 844−845.
(218) Sprenger, S. Epoxy Resin Composites with Surface-modified Silicon Dioxide Nanoparticles: A Review. *J. Appl. Polym. Sci.* **2013**, *130* (3), 1421−1428.
(219) Nakamura, Y.; Yamaguchi, M.; Okubo, M.; Matsumoto, T. Effect of Particle Size on the Fracture Toughness of Epoxy Resin Filled with Spherical Silica. *Polymer* **1992**, *33* (16), 3415−3426.
(220) Johnsen, B. B.; Kinloch, A. J.; Mohammed, R. D.; Taylor, A. C.; Sprenger, S. Toughening Mechanisms of Nanoparticle-modified Epoxy Polymers. *Polymer* **2007**, *48* (2), 530−541.
(221) Liu, H. Y.; Wang, G. T.; Mai, Y. W.; Zeng, Y. on Fracture Toughness of Nano-particle Modified Epoxy. *Composites, Part B* **2011**, *42* (8), 2170−2175.
(222) Dittanet, P.; Pearson, R. A. Effect of Silica Nanoparticle Size on Toughening Mechanisms of Filled Epoxy. *Polymer* **2012**, *53* (9), 1890−1905.
(223) Lin, B.; Zhao, L. G.; Tong, J. A Crystal Plasticity Study of Cyclic Constitutive Behaviour, Crack-tip Deformation and Crack-growth Path for a Polycrystalline Nickel-based Superalloy. *Eng. Fract. Mech.* **2011**, *78* (10), 2174−2192.
(224) Liao, Y. S.; Li, Y. B.; Huang, M. H.; Wang, B. S.; Yang, Y. C.; Pei, S. K. Effect of Hole Relative Size and Position on Crack Deflection Angle of Repaired Structure. *Theor. Appl. Fract. Mech.* **2019**, *101*, 92−102.
(225) Wang, M.; Zhao, L.; Fourmeau, M.; Nelias, D. Crack Plane Deflection and Shear Wave Effects in the Dynamic Fracture of Silicon Single Crystal. *J. Mech. Phys. Solids.* **2019**, *122*, 472−488.
(226) Sassoni, E.; Andreotti, S.; Bellini, A.; Mazzanti, B.; Bignozzi, M. C.; Mazzotti, C.; Franzoni, E. Influence of Mechanical Properties, Anisotropy, Surface Roughness and Porosity of Brick on FRP Debonding Force. *Composites, Part B* **2017**, *108*, 257−269.
(227) Kabel, J.; Yang, Y.; Balooch, M.; Howard, C.; Koyanagi, T.; Terrani, K. A.; Katoh, Y.; Hosemann, P. Micro-mechanical Evaluation of SiC-SiC Composite Interphase Properties and Debond Mechanisms. *Composites, Part B* **2017**, *131*, 173−183.
(228) Wang, P. P.; Maeda, R.; Aoki, M.; Kubozono, T.; Yoshihara, D.; Shundo, A.; Kobayashi, T.; Yamamoto, S.; Tanaka, K.; Yamada, S. In Situ Transmission Electron Microscopy Observation of the Deformation and Fracture Processes of an Epoxy/Silica Nanocomposite. *Soft Matter* **2022**, *18* (6), 1149−1153.
(229) Soni, N. J.; Lin, P. H.; Khare, R. Effect of Cross-linker Length on the Thermal and Volumetric Properties of Cross-linked Epoxy Networks: A Molecular Simulation Study. *Polymer* **2012**, *53* (4), 1015−1019.
(230) Mijovic, J.; Zhang, H. Local Dynamics and Molecular Origin of Polymer Network-water Interactions as Studied by Broadband Dielectric Relaxation Spectroscopy, FTIR, and Molecular Simulations. *Macromolecules* **2003**, *36* (4), 1279−1288.
(231) Shenogina, N. B.; Tsige, M.; Patnaik, S. S.; Mukhopadhyay, S. M. Molecular Modeling Approach to Prediction of Thermo-mechanical Behavior of Thermoset Polymer Networks. *Macromolecules* **2012**, *45* (12), 5307−5315.
(232) Okabe, T.; Oya, Y.; Tanabe, K.; Kikugawa, G.; Yoshioka, K. Molecular Dynamics Simulation of Crosslinked Epoxy Resins: Curing and Mechanical Properties. *Eur. Polym. J..* **2016**, *80*, 78−88.
(233) Odegard, G. M.; Patil, S. U.; Deshpande, P. P.; Kanhaiya, K.; Winetrout, J. J.; Heinz, H.; Shah, S. P.; Maiaru, M. Molecular Dynamics Modeling of Epoxy Resins Using the Reactive Interface Force Field. *Macromolecules* **2021**, *54* (21), 9815−9824.
(234) Andrews, E. H.; Kinloch, A. J. Mechanics of Adhesive Failure. II. *Proc. R. Soc. London A* **1973**, *332* (1590), 401−414.
(235) Bahlakeh, G.; Ramezanzadeh, B. A Detailed Molecular Dynamics Simulation and Experimental Investigation on the Interfacial Bonding Mechanism of an Epoxy Adhesive on Carbon Steel Sheets Decorated with a Novel Cerium-lanthanum Nanofilm. *ACS Appl. Mater. Interfaces* **2017**, *9* (20), 17536−17551.
(236) Okamoto, K.; Ganbe, T.; Sekine, N.; Aoki, M.; Inutsuka, M.; Shundo, A.; Kawaguchi, D.; Tanaka, K. Nanoscale Characterization of Epoxy Interface on Silica. *IEEE Int. Conf. Dielectrics* **2016**, 84−87.
(237) Munz, M.; Sturm, H.; Schulz, E. Interphase Characterization via the Stiffness Contrast of a Scanning Force Microscope in Displacement Modulation Mode. *Surf. Interface Anal.* **2000**, *30* (1), 410−414.
(238) Munz, M.; Sturm, H.; Stark, W. Mechanical Gradient Interphase by Interdiffusion and Antiplasticisation Effect - Study of an Epoxy/Thermoplastic System. *Polymer* **2005**, *46* (21), 9097−9112.
(239) Turunen, M. P. K.; Marjamaki, P.; Paajanen, M.; Lahtinen, J.; Kivilahti, J. K. Pull-off Test in the Assessment of Adhesion at Printed Wiring Board Metallisation/Epoxy Interface. *Microelectron. Reliab.* **2004**, *44* (6), 993−1007.
(240) Watts, J. F.; Castle, J. E.; Ludlam, S. J. The Orientation of Molecules at the Locus of Failure of Polymer-coatings on Steel. *J. Mater. Sci.* **1986**, *21* (8), 2965−2971.
(241) Bockenheimer, C.; Valeske, B.; Possart, W. Network Structure in Epoxy Aluminium Bonds after Mechanical Treatment. *Int. J. Adhes. Adhes.* **2002**, *22* (5), 349−356.
(242) Onard, S.; Martin, I.; Chailan, J. F.; Crespy, A.; Carriere, P. Nanostructuration in Thin Epoxy-amine Films Inducing Controlled Specific Phase Etherification: Effect on the Glass Transition Temperatures. *Macromolecules* **2011**, *44* (9), 3485−3493.
(243) Chung, J.; Munz, M.; Sturm, H. Stiffness Variation in the Interphase of Amine-cured Epoxy Adjacent to Copper Micro-structures. *Surf. Interface Anal.* **2007**, *39* (7), 624−633.
(244) Aufray, M.; Roche, A. Properties of the Interphase Epoxy-amine/Metal: Influences from the Nature of the Amine and the Metal. In *Adhesion-Current Research and Application*; Possart, W., Ed.; Wiley-VCH, 2005; pp 89−102.
(245) Marsh, J.; Minel, L.; Barthes-Labrousse, M. G.; Gorse, D. Interaction of Epoxy Model Molecules with Aluminium, Anodised Titanium and Copper Surfaces: An XPS Study. *Appl. Surf. Sci.* **1998**, *133* (4), 270−286.
(246) Roche, A. A.; Bouchet, J.; Bentadjine, S. Formation of Epoxy-diamine/Metal Interphases. *Int. J. Adhes. Adhes.* **2002**, *22* (6), 431−441.
(247) Possart, W.; Kruger, J. K.; Wehlack, C.; Muller, U.; Petersen, C.; Bactavatchalou, R.; Meiser, A. Formation and Structure of Epoxy Network Interphases at the Contact to Native Metal Surfaces. *CR Chim.* **2006**, *9* (1), 60−79.
(248) Deng, S. Q.; Djukic, L.; Paton, R.; Ye, L. Thermoplastic-epoxy Interactions and Their Potential Applications in Joining Composite Structures - A Review. *Composites, Part A* **2015**, *68*, 121−132.
(249) Hirai, T.; Kawasaki, K.; Tanaka, K. Interfacial Kinetics of a Model Epoxy-amine Addition Reaction. *Phys. Chem. Chem. Phys.* **2012**, *14* (39), 13532−13534.
(250) Bentadjine, S.; Petiaud, R.; Roche, A. A.; Massardier, V. Organo-metallic Complex Characterization Formed When Liquid Epoxy-diamine Mixtures Are Applied onto Metallic Substrates. *Polymer* **2001**, *42* (14), 6271−6282.
(251) Karasinski, E. N.; Da Luz, M. G.; Lepienski, C. M.; Coelho, L. A. F. Nanostructured Coating Based on Epoxy/Metal Oxides: Kinetic Curing and Mechanical Properties. *Thermochim. Acta* **2013**, *569*, 167−176.
(252) Meiser, A.; Kubel, C.; Schafer, H.; Possart, W. Electron Microscopic Studies on the Diffusion of Metal Ions in Epoxy-metal Interphases. *Int. J. Adhes. Adhes.* **2010**, *30* (3), 170−177.
(253) Liu, Y.; Hamon, A. L.; Haghi-Ashtiani, P.; Reiss, T.; Fan, B. H.; He, D. L.; Baio, J. B. Quantitative Study of Interface/Interphase in

Epoxy/Graphene-based Nanocomposites by Combining STEM and EELS. *ACS Appl. Mater. Interfaces* **2016**, *8* (49), 34151−34158.

(254) Aoki, M.; Shundo, A.; Okamoto, K.; Ganbe, T.; Tanaka, K. Segregation of an Amine Component in a Model Epoxy Resin at a Copper Interface. *Polym. J.* **2019**, *51* (3), 359−363.

(255) Yamamoto, S.; Kuwahara, R.; Aoki, M.; Shundo, A.; Tanaka, K. Molecular Events for an Epoxy-amine System at a Copper Interface. *ACS Appl. Polym. Mater.* **2020**, *2* (4), 1474−1481.

(256) Yamamoto, S.; Tanaka, K. Entropy-driven Segregation in Epoxy-amine Systems at a Copper Interface. *Soft Matter* **2021**, *17* (5), 1359−1367.

(257) Unnikrishnan, K. P.; Thachil, E. T. Toughening of Epoxy Resins. *Des. Monomers Polym.* **2006**, *9* (2), 129−152.

(258) Wang, X. S.; Kim, H. K.; Fujita, Y.; Sudo, A.; Nishida, H.; Endo, T. Relaxation and Reinforcing Effects of Polyrotaxane in an Epoxy Resin Matrix. *Macromolecules* **2006**, *39* (3), 1046−1052.

(259) Pruksawan, S.; Samitsu, S.; Yokoyama, H.; Naito, M. Homogeneously Dispersed Polyrotaxane in Epoxy Adhesive and Its Improvement in the Fracture Toughness. *Macromolecules* **2019**, *52* (6), 2464−2475.

(260) Hanafusa, A.; Ando, S.; Ozawa, S.; Ito, M.; Hasegawa, R.; Mayumi, K.; Ito, K. Viscoelastic Relaxation Attributed to the Molecular Dynamics of Polyrotaxane Confined iin an Epoxy Resin Network. *Polymer J.* **2020**, *52* (10), 1211−1221.

(261) Tano, K.; Sato, E. Synthesis and Dissociation Behavior of Degradable Network Polymers Consisting of Epoxides and 9-Anthracene Carboxylic Acid Dimer. *Chem. Lett.* **2021**, *50* (10), 1787−1790.

(262) Takahashi, A.; Ohishi, T.; Goseki, R.; Otsuka, H. Degradable Epoxy Resins Prepared from Diepoxide Monomer with Dynamic Covalent Disulfide Linkage. *Polymer* **2016**, *82* (1), 319−326.

(263) Ruiz de Luzuriaga, A.; Matxain, J. M.; Ruiperez, F.; Martin, R.; Asua, J. M.; Cabanero, G.; Odriozola, I. Transient Mechanochromism in Epoxy Vitrimer Composites Containing Aromatic Disulfide Crosslinks. *J. Mater. Chem. C* **2016**, *4* (26), 6220−6223.

(264) Mo, R. B.; Hu, J.; Huang, H. W.; Sheng, X. X.; Zhang, X. Y. Tunable, Self-healing and Corrosion Inhibiting Dynamic Epoxy-polyimine Network Built by Post-crosslinking. *J. Mater. Chem. A* **2019**, *7* (7), 3031−3038.

(265) Montarnal, D.; Capelot, M.; Tournilhac, F.; Leibler, L. Silica-like Malleable Materials from Permanent Organic Networks. *Science* **2011**, *334* (6058), 965−968.

(266) Capelot, M.; Unterlass, M. M.; Tournilhac, F.; Leibler, L. Catalytic Control of the Vitrimer Glass Transition. *ACS Macro Lett.* **2012**, *1* (7), 789−792.

(267) Chen, M.; Zhou, L.; Wu, Y. P.; Zhao, X. L.; Zhang, Y. J. Rapid Stress Relaxation and Moderate Temperature of Malleability Enabled by the Synergy of Disulfide Metathesis and Carboxylate Trans-esterification in Epoxy Vitrimers. *ACS Macro Lett.* **2019**, *8* (3), 255−260.

(268) Yang, Y.; Xu, Y.; Ji, Y.; Wei, Y. Functional Epoxy Vitrimers and Composites. *Prog. Mater. Sci.* **2021**, *120* (6), 100710.

(269) Yang, Z.; Wang, Q.; Wang, T. Dual-triggered and Thermally Reconfigurable Shape Memory Graphene-vitrimer Composites. *ACS Appl. Mater. Interfaces* **2016**, *8* (33), 21691−21699.

(270) Yang, Y.; Pei, Z.; Zhang, X.; Tao, L.; Wei, Y.; Ji, Y. Carbon Nanotube-vitrimer Composite for Facile and Efficient Photo-welding of Epoxy. *Chem. Sci.* **2014**, *5* (9), 3486−3492.

(271) Sun Lee, W.; Yu, J. Comparative Study of Thermally Conductive Fillers in Underfill for the Electronic Components. *Diamond Relat. Mater.* **2005**, *14* (10), 1647−1653.

(272) Choi, S.; Kim, J. Thermal Conductivity of Epoxy Composites with a Binary-particle System of Aluminum Oxide and Aluminum Nitride Fillers. *Composites, Part B* **2013**, *51*, 140−147.

(273) Shi, Z. Q.; Radwan, M.; Kirihara, S.; Miyamoto, Y.; Jin, Z. H. Enhanced Thermal Conductivity of Polymer Composites Filled with Three-dimensional Brushlike ALN Nanowhiskers. *Appl. Phys. Lett.* **2009**, *95* (22), 224104.

(274) Li, T. L.; Hsu, S. L. C. Enhanced Thermal Conductivity of Polyimide Films via a Hybrid of Micro- and Nano-sized Boron Nitride. *J. Phys. Chem. B* **2010**, *114* (20), 6825−6829.

(275) Wang, Q.; Chen, X.; Huang, X.; Muhammad, A.; Shi, Y.; Dai, C.; Ren, N.; Paramane, A. Tailoring Electric Field Distortion in High-voltage Power Modules Utilizing Epoxy Resin/Silicon Carbide Whisker Composites with Field-dependent Conductivity. *ACS Appl. Electron. Mater.* **2022**, *4* (1), 478−493.

(276) Cahill, D. G.; Watson, S. K.; Pohl, R. O. Lower Limit to the Thermal Conductivity of Disordered Crystals. *Phys. Rev. B* **1992**, *46* (10), 6131−6140.

(277) Xu, Y.; Wang, X.; Zhou, J.; Song, B.; Jiang, Z.; Lee, E. M. Y.; Huberman, S.; Gleason, K. K.; Chen, G. Molecular Engineered Conjugated Polymer with High Thermal Conductivity. *Sci. Adv.* **2018**, *4* (3), No. eaar3031.

(278) Maeda, R.; Okuhara, K.; Nakamura, A.; Hayakawa, T.; Uehara, Y.; Motoya, T.; Nobutoki, H. Higher-order-structure Formation in Liquid Crystal Epoxy Thermosets Investigated by Synchrotron Radiation Wide-angle X-ray Diffraction. *Chem. Lett.* **2016**, *45* (7), 795−797.

(279) Lv, G.; Jensen, E.; Evans, C. M.; Cahill, D. G. High Thermal Conductivity Semicrystalline Epoxy Resins with Anthraquinone-based Hardners. *ACS Appl. Polym. Mater.* **2021**, *3* (9), 4430−4435.

(280) Mo, H. L.; Huang, X. Y.; Liu, F.; Yang, K.; Li, S. T.; Jiang, P. K. Nanostructured Electrical Insulating Epoxy Thermosets with High Thermal Conductivity, High Thermal Stability, High Glass Transition Temperatures and Excellent Dielectric Properties. *IEEE Trans. Dielectr. Electr. Insul.* **2015**, *22* (2), 906−915.

(281) Song, S. H.; Katagi, H.; Takezawa, Y. Study on High Thermal Conductivity of Mesogenic Epoxy Resin with Spherulite Structure. *Polymer* **2012**, *53* (20), 4489−4492.

(282) Harada, M.; Ochi, M.; Tobita, M.; Kimura, T.; Ishigaki, T.; Shimoyama, N.; Aoki, H. Thermal-conductivity Properties of Liquid-crystalline Epoxy Resin Cured under a Magnetic Field. *J. Polym. Sci., Part B: Polym. Phys.* **2003**, *41* (14), 1739−1743.

(283) Cheng, W. T.; Chih, Y. W.; Yeh, W. T. In Situ Fabrication of Photocurable Conductive Adhesives with Silver Nano-particles in the Absence of Capping Agent. *Int. J. Adhes. Adhes.* **2007**, *27* (3), 236−243.

(284) Martin-Gallego, M.; Lopez-Manchado, M. A.; Calza, P.; Roppolo, I.; Sangermano, M. Gold-functionalized Graphene as Conductive Filler in UV-curable Epoxy Resin. *J. Mater. Sci.* **2015**, *50* (2), 605−610.

(285) Lee, H. H.; Chou, K. S.; Shih, Z. W. Effect of Nano-sized Silver Particles on the Resistivity of Polymeric Conductive Adhesives. *Int. J. Adhes. Adhes.* **2005**, *25* (5), 437−441.

(286) Yim, M. J.; Paik, K. W. Recent Advances on Anisotropic Conductive Adhesives (ACAs) for Flat Panel Displays and Semi-conductor Packaging Applications. *Int. J. Adhes. Adhes.* **2006**, *26* (5), 304−313.

(287) Mir, I.; Kumar, D. Recent Advances in Isotropic Conductive Adhesives for Electronics Packaging Applications. *Int. J. Adhes. Adhes.* **2008**, *28* (7), 362−371.

(288) Li, Y.; Wong, C. P. Recent Advances of Conductive Adhesives as a Lead-free Alternative in Electronic Packaging: Materials, Processing, Reliability and Applications. *Mater. Sci. Eng. R Rep.* **2006**, *51* (1−3), 1−35.

(289) Wu, H. P.; Liu, J. F.; Wu, X. J.; Ge, M. Y.; Wang, Y. W.; Zhang, G. Q.; Jiang, J. Z. High Conductivity of Isotropic Conductive Adhesives Filled with Silver Nanowires. *Int. J. Adhes. Adhes.* **2006**, *26* (8), 617−621.

(290) Jiang, H. J.; Yim, M. J.; Lin, W.; Wong, C. P. Novel Nonconductive Adhesives/Films with Carbon Nanotubes for High-performance Interconnects. *IEEE Trans. Compon. Packag. Technol.* **2009**, *32* (4), 754−758.

(291) Massoumi, B.; Hosseinzadeh, M.; Jaymand, M. Electrically Conductive Nanocomposite Adhesives Based on Epoxy or Chlor-oprene Containing Polyaniline, and Carbon Nanotubes. *J. Mater. Sci.: Mater. Electron.* **2015**, *26* (8), 6057−6067.

https://doi.org/10.1021/jacsau.2c00120
JACS Au 2022, 2, 1522−1542

(292) Ng, F. F.; Couture, G.; Philippe, C.; Boutevin, B.; Caillol, S. Bio-based Aromatic Epoxy Monomers for Thermoset Materials. *Molecules* **2017**, *22* (1), 149.
(293) Wang, X.; Guo, W. W.; Song, L.; Hu, Y. Intrinsically Flame Retardant Bio-based Epoxy Thermosets: A Review. *Composites, Part B* **2019**, *179*, 107487.
(294) Auvergne, R.; Caillol, S.; David, G.; Boutevin, B.; Pascault, J. P. Biobased Thermosetting Epoxy: Present and Future. *Chem. Rev.* **2014**, *114* (2), 1082−1115.
(295) Baroncini, E. A.; Yadav, S. K.; Palmese, G. R.; Stanzione, J. F. Recent Advances in Bio-based Epoxy Resins and Bio-based Epoxy Curing Agents. *J. Appl. Polym. Sci.* **2016**, *133* (45), 44103.
(296) Yue, L.; Liu, F.; Mekala, S.; Patel, A.; Gross, R. A.; Manas-Zloczower, I. High Performance Biobased Epoxy Nanocomposite Reinforced with a Bacterial Cellulose Nanofiber Network. *ACS Sustainable Chem. Eng.* **2019**, *7* (6), 5986−5992.
(297) Wang, Z.; Gnanasekar, P.; Sudhakaran Nair, S.; Farnood, R.; Yi, S.; Yan, N. Biobased Epoxy Synthesized from a Vanillin Derivative and Its Reinforcement Using Lignin-containing Cellulose Nanofibrils. *ACS Sustainable Chem. Eng.* **2020**, *8* (30), 11215−11223.

Recommended by ACS

Effects of Dynamic Disulfide Bonds on Mechanical Behavior in Glassy Epoxy Thermosets

Broderick Lewis, Kenneth R. Shull, *et al.*
MARCH 13, 2023
ACS APPLIED POLYMER MATERIALS

Preparation of Hydrophobic Low-*k* Epoxy Resins with High Adhesion Using a Benzocyclobutene-Rosin Modifier

Fei Fu, Jie Song, *et al.*
APRIL 05, 2023
ACS SUSTAINABLE CHEMISTRY & ENGINEERING

Closed-Loop Recycling of Carbon Fiber-Reinforced Composites Enabled by a Dual-Dynamic Cross-linked Epoxy Network

Yingying Liu, Zhen Hu, *et al.*
JANUARY 19, 2023
ACS SUSTAINABLE CHEMISTRY & ENGINEERING

High Mechanical Strength of Shape-Memory Hyperbranched Epoxy Resins

Yanfen Lu, Daohong Zhang, *et al.*
JULY 13, 2022
ACS APPLIED POLYMER MATERIALS

Get More Suggestions >

https://doi.org/10.1021/jacsau.2c00120
JACS Au 2022, 2, 1522−1542